Polarforschung 78 (1-2), 29 – 51, 2008 (erschienen 2009)

Polar Climate Modelling: Regional Feedbacks and Global Links – an IPY Approach –

by Klaus Dethloff[1]*, Annette Rinke[1], Dörthe Handorf[1], Wolfgang Dorn[1], Sascha Brand[1], Matthias Läuter[1], Subodh K. Saha[1], Elena Sokolova[1] and Ksenya Glushak[1]

Abstract: Global climate models (GCMs) constitute the primary tool for capturing the behaviour of the Earth's climate system. Regional climate model (RCM) systems with high spatial and temporal resolution and improved physics in polar regions are more accurate than GCMs with relatively low resolution. RCMs can provide added value at small scales to the climate statistics when driven by GCM outputs at the lateral and lower boundaries, assuming that GCMs are accurate on large scales. Any advances in regional climate modelling must be based on analysis of physical processes in comparison with observations, which is rather difficult in data sparse areas like the polar regions, where RCMs are often used as intelligent data interpolator. RCMs can be used as a testbed for the development of improved and more adequate parameterization of important sub-grid scale processes, for the reduction of shortcomings of the used numerical methods, for the choice of the horizontal and vertical resolution, for the quantification of uncertainties in the boundary forcing connected with low-frequency variability in the driving data, for the treatment of the boundary forcing, for the choice of the regional model domain with size and position, for the nesting hierarchy, for the study of internal model variability and for the choice of climate change scenarios. In this way, RCMs can deliver valuable input for improving the performance of global climate models, especially in the Arctic. The use of an ensemble approach of different models with standardised conditions is an accepted model set-up for studying different model realisations of the same climate conditions and for analysing the uncertainty ranges. Uncertainty ranges derived in this manner could be of great importance for the reliability and robustness of regional climate change scenarios for the Arctic. The influences of atmosphere–ocean–sea-ice and atmosphere–land–soil interactions in coupled RCM simulations driven either by European reanalyses (ERA-40) or GCM boundary forcing data have been investigated. These deliver valuable information by improving the physical realism of the considered feedback processes and for quantifying the uncertainty range of Arctic RCM simulations with respect to tuned parameters. The global impact of an improved sea ice albedo parameterization, tested in a RCM setup, and the global influences of interactive stratospheric chemistry in the Arctic polar vortex have been investigated. The need for new dynamical model cores with two-way feedbacks is discussed.

Zusammenfassung: Globale Klimamodelle (GCMs) bilden das primäre Hilfsmittel für die Erfassung des Verhaltens des Klimasystems der Erde. Regionale Klimamodellsysteme (RCM) mit hoher räumlicher und zeitlicher Auflösung und verbesserter Physik in Polargebieten sind genauer als GCMs mit relativ geringer Auflösung. RCMs können auf kleinen Skalen einen zusätzlichen Wert zur Klimastatistik liefern, wenn sie mit GCM-Ausgaben an den seitlichen und unteren Rändern angetrieben werden, angenommen, dass GCMs auf großen Skalen genau sind. Jeder Fortschritt in der regionalen Klimamodellierung muss auf der Analyse physikalischer Prozesse im Vergleich mit Beobachtungen beruhen, was in datenarmen Gebieten wie den Polargebieten, wo RCMs häufig als intelligenter Dateninterpolator verwendet werden, ziemlich schwierig ist. RCMs können als Testumgebung für die Entwicklung verbesserter und genauerer Parametrisierungen wichtiger unterhalb der Gitterauflösung liegender Prozesse, für die Reduzierung von Defiziten in den verwendeten numerischen Methoden, für die Wahl der Unsicherheiten im Randantrieb in Verbindung mit niederfrequenter Variabilität in den Antriebsdaten, für die Behandlung des Randantriebs, für die Wahl des regionalen Modellgebiets mit Größe und Lage, für die Schachtelungshierarchie, für die Untersuchung interner Modellvariabilität und für die Wahl von Klimaänderungsszenarien verwendet werden. Auf diese Weise können RCMs einen wertvollen Beitrag zur Verbesserung der Leistungsfähigkeit globaler Klimamodelle liefern, speziell in der Arktis. Die Verwendung eines Ensemble-Ansatzes von verschiedenen Modellen mit standardisierten Bedingungen ist eine anerkannte Modell-Anordnung für die Untersuchung unterschiedlicher Modellrealisierungen der gleichen Klimabedingungen und für die Analyse des Unsicherheitsbereichs. Auf diese Weise abgeleitete Unsicherheitsbereiche könnten von großer Bedeutung für die Glaubwürdigkeit und Robustheit regionaler Klimaänderunsszenarien der Arktis sein. Die Einflüsse von Atmosphäre–Ozean–Meereis- und Atmosphäre–Land–Boden-Wechselwirkungen in gekoppelten RCM-Simulationen, entweder angetrieben durch Europäische Reanalysen (ERA-40) oder GCM-Randantriebsdaten, sind untersucht worden. Diese liefern wertvolle Informationen durch die Verbesserung des physikalischen Realismus der betrachteten Rückkoppelungsprozesse und für die Quantifizierung des Unsicherheitsbereichs arktischer RCM-Simulationen in Bezug auf abgestimmte Parameter. Die globale Auswirkung einer verbesserten Meereisalbedo-Parametrisierung, getestet in einer RCM-Anordnung, und die globalen Einflüsse einer interaktiven stratosphärischen Chemie im arktischen Polarwirbel sind untersucht worden. Der Bedarf an neuen dynamischen Modellkernen mit wechselseitigen Rückkoppelungen wird diskutiert.

INTRODUCTION

Rapidly changing Arctic climate with a vigorous decline of sea-ice area in 2007 and unprecedented warming of the Arctic atmosphere, ocean and land have attracted attention of the international scientific community representing all geosciences disciplines. The extreme Arctic changes have coincided with the International Polar Year (IPY, 2007/08) with its enhanced observation activities in the Arctic and there is a hope that the "Arctic change of the 2000s" will be documented in greater details.

Polar regions are key players in the climate system because of the strong modification of the surface-energy budget through snow and ice cover, which is tightly coupled to the global circulation of the atmosphere and the ocean. The climate of the Arctic is already subject to visible changes and the sea-ice albedo feedback-mechanism acts as an amplifier of climate change. The observed decrease of Arctic summer sea-ice cover over the last decades is best viewed as a combination of strong natural variability due to large-scale dynamics and regional feedbacks in the coupled ice–ocean–atmosphere system and a growing radiative forcing associated with rising concentrations of atmospheric greenhouse gases. The attribution of ongoing changes in the Arctic is more difficult than in the Antarctic because natural variability is larger, masking the evidence of anthropogenic influences.

In order to explain changes in the polar climate and predict future dynamics of the polar transformations we need models of the Arctic and Antarctic climatic systems, able to reproduce past and present states, variability and trends and predict future changes of the major polar environmental parameters. In general, existing models are capable to do this job but their results are not always satisfactory. STROEVE et al. (2007) and

[1] Alfred Wegener Institute for Polar and Marine Research, Research Unit Potsdam, Telegrafenberg A43, 14473 Potsdam, Germany.
* Corresponding author <Klaus.Dethloff@awi.de>

Manuscript received 22 September 2008; accepted 01 October 2008

SERREZE et al. (2007) have shown that Arctic sea ice declines faster than predicted by models participating in the Intergovernmental Panel on Climate Change (IPCC) Fourth Assessment Report (see CHRISTENSEN et al. 2007), because there is a significant level of uncertainties associated with model forcing, parameterization of physical processes and numerous nonlinear feedbacks and interactions and tuned model parameters based on existing observational data. Therefore a main question is how to reduce the uncertainties in model results and how to provide best linkages among model and observational needs?

Observations and connections to models

It is difficult to construct, understand, and explain changes in the climate system based on observational data without modelling. On the other hand, it is useless to employ models for this purpose and for projection of climate change without model validation, e.g. determination of model errors and their uncertainties. Observational data analysis is needed for model calibration and validation. For example, small errors in ice parameters stemming from errors in atmospheric forcing can translate into serious errors in ocean variables through an uncertainty cascade. There are not enough observational data for regional model initialization, forcing, validation and assimilation.

A comprehensive sustained Arctic Observational Network (AON) has been suggested, to satisfy needs of both observational and modelling communities, described by the committee on designing an AON (2006). On the other hand, modelling has to play a substantial role in the design of AON and to provide a scientifically effective and representative system for the temporal and spatial distribution of observational sites for operational forecasts and for studies associated with long-term system variability. Observations are highly integrated variables, e.g. precipitation represents very complex feedbacks. Therefore, the interpretation of observations needs models with complex enough realism at the process level, which are not available.

The improvement of GCMs depends also on the availability of high quality atmospheric measurements. For this purpose, high-resolution observations over long periods and over long distances are required. Regular long-term observations at selected stations and satellite data provide a general picture of the temporal atmospheric development, while detailed spatial measurements can be obtained by regular airborne measurements. Atmospheric measurements of surface energy balance, heat and moisture fluxes, cloud and aerosol properties, aerological, water vapour and ozone profiles are essential for the understanding of key processes in the Arctic climate system.

Major gaps and uncertainties exist in our knowledge of processes governing the build-up of aerosols in the Arctic and its role for climate change. Various anthropogenic and natural sources contribute, including increased tundra fires. Atmospheric aerosol and clouds have a mutual influence on each other. Aerosol particles modify many climatically important cloud properties, including the cloud reflectivity and lifetime. Aerosol optical properties enter radiation transfer calculations, and the aerosol-cloud interactions are important for the parameterization of cloud formation processes.

Strong stratospheric ozone losses have been found in some of the Arctic winters. Anthropogenic chemical loss of ozone and natural dynamically driven variability contribute each about half to the overall variability of total ozone in the Arctic in spring. To allow reliable predictions of ozone abundances over the Arctic for the next half-century, a solid understanding of both factors is needed and how they may change in a scenario of increasing greenhouse-gas levels and decreasing halogen loading of the stratosphere. Observational results show that changes in the temperature conditions in the Arctic polar stratosphere have been a major driver of large Arctic ozone losses during the past decade.

Long-term observations and process studies on drifting sea ice camps, airborne and satellite observations of the lower and free troposphere, the snow covered sea ice and the upper Arctic Ocean are needed to reduce the uncertainties connected with the disappearance of Arctic sea ice in summer. As part of observations during the International Polar Year (IPY) the Russian North Pole drifting station NP-35 was build by the Arctic and Antarctic Research Institute (AARI) St. Petersburg on an ice floe in the north of Severnaya Zemlya islands. From 18th September 2007 until 12th July 2008 NP-35 drifted over the Arctic Ocean to Svalbard. In order to understand the interaction between ocean, sea ice and the atmospheric boundary layer, continuous measurements have been carried out from September 2007 until July 2008, including sea ice thickness measurements, standard meteorological parameters, surface radiation budget, atmospheric soundings and measurements of vertical ozone profiles. Atmospheric measurements based on tethered balloons and radio and ozone sondes have been carried out to measure vertical profiles of air temperature, relative humidity, wind speed, wind direction and ozone in the planetary boundary layer and the free tropo- and lower stratosphere.

Model validation and RCM improvements

The measurements at NP-35 will be compared with simulations based on the atmospheric regional climate model HIRHAM, following the approach by RINKE et al. (2006) developed for the SHEBA data set in the pan-Arctic integration domain (Fig. 1a). Beside RCMs, a single-column model (SCM) approach, which is essentially an isolated column of a RCM or GCM, can be used to improve parameterizations of clouds and radiation or planetary boundary layer turbulence schemes used in climate models. This goal is being achieved through the use of field measurements to evaluate the parameterizations. This approach has been applied by DETHLOFF et al. (2001) for the Arctic and needs a careful determination of the nonlinear advection terms influencing the processes in the column.

To solve the problem of discontinuous, spatially incomplete meteorological records in polar regions and across the globe, global reanalyses were developed in which a fixed assimilation scheme is used to incorporate past observations into an atmospheric numerical weather prediction model. As such, a reanalysis produces a large number of variables on a uniformly spaced grid. For validation purposes RCMs are driven by global reanalyses data.

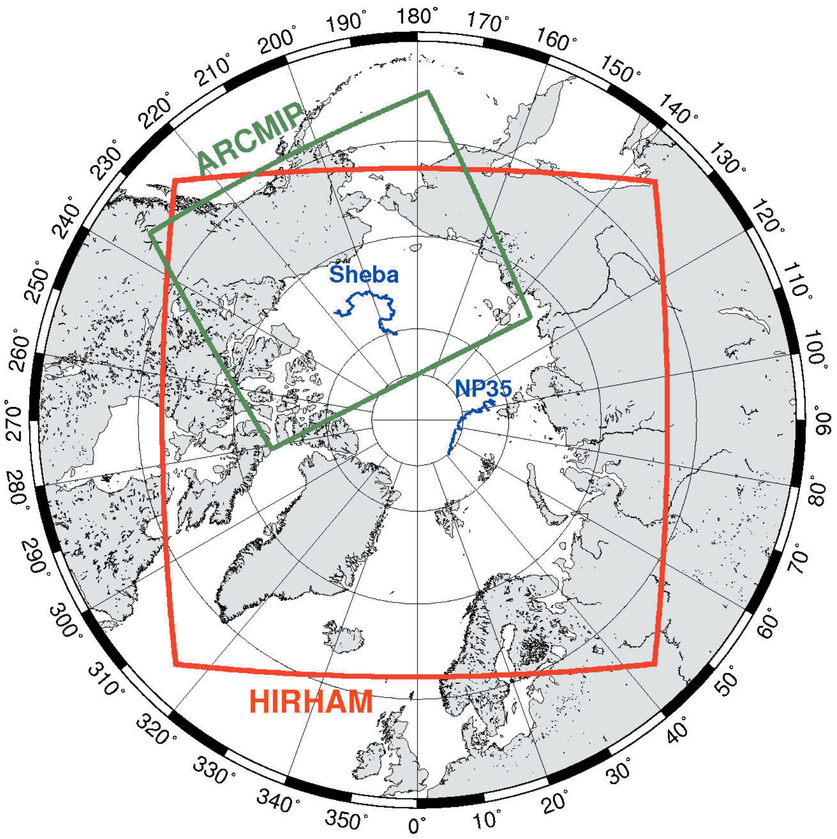

Fig. 1a: The integration domain of the Arctic Regional Climate Model Intercomparison Project (ARCMIP, green), the trajectory of the ice camp during the Surface Heat Budget of the Arctic Ocean campaign (SHEBA, blue), the pan-Arctic integration domain of the regional climate model HIRHAM (red), and the trajectory of the Russian ice floe station NP-35 (blue).

Abb. 1a: Das Integrationsgebiet des „Arctic Regional Climate Model Intercomparison Project“ (ARCMIP, grün), die Trajektorie des Eislagers während der „Surface Heat Budget of the Arctic Ocean“-Kampagne (SHEBA, blau), das gesamtarktische Integrationsgebiet des regionalen Klimamodells HIRHAM (rot) und die Trajektorie der russischen Eisschollen-Station NP-35 (blau).

Bromwich et al. (2007) have presented a wide array of recent knowledge regarding the status of the major global reanalyses (NCEP/NCAR global reanalysis, JRA-25 Japan Meteorological Agency and Central Research Institute reanalyses, European reanalyses ERA-40) in the polar regions. The skill of different reanalyses products is much higher in the Arctic than the Antarctic, where the reanalyses are only reliable in the summer months prior to the modern satellite era.

Since many physical processes occurring in polar region are still not well understood, it is not surprising that simulated climates of the Arctic vary widely, depending on the choice of climate model and physical parameterizations. Large variations have been found among the GCM simulations of Arctic sea-level pressure, surface temperature, precipitation, and cloud cover. The representation of polar processes in GCMs is rather poor.

RCMs are limited-area models that are driven at their lateral boundaries by reanalyses or GCM-generated data (e.g., Giorgi 1991). The prognostic variables in a RCM are relaxed towards these lateral boundary conditions in a boundary zone of some grid rows towards margins of the domain, following a scheme of Davies (1976). The results near these margins may be unrealistic due to the nesting procedure and are not considered in the analysis. It should be realised that in the latter procedure, potential systematic errors in the GCM are transferred to the RCM.

The use of RCMs is well accepted in order to improve the parameterizations of polar processes, the representation of high-latitude processes and the potential impact on climate simulations. The modelling strategy is based on the quantitative evaluation of individual model components and process parameterizations. Further, model sensitivities are assessed and coupling strategies and coupled processes are investigated. Observational field and process studies, which should lead to improved parameterizations of Arctic specific processes are carried out on a much finer scale than current GCMs can resolve. The adaptation of this meso-scale information to a global-scale parameterization is a complex and difficult topic.

RCMs can contribute to this issue by dynamical downscaling with higher horizontal and vertical resolution compared to the driving data. Such models improve the understanding of feedbacks by process studies in close connection with observations and by upscaling regionally important processes in global models, e.g. connected with sub-grid scale parameterizations, albedo effects and coupled feedbacks. The use of RCMs with specified “perfect” lateral boundary conditions eliminates problems originating from lower latitudes in contaminating the results in the Arctic. Further, deficiencies of GCMs in describing the Arctic climate are at least partly due to inadequate parameterizations of important Arctic physical processes. Recent RCM studies have indicated the importance of accurate representation of momentum, heat and moisture exchange in the PBL (Dethloff et al. 2001, Tjernström et al. 2005), surface albedo (Køltzow et al. 2003), cloud-radiation interaction (Cassano et al. 2001, Bromwich et al. 2001, Girard & Blanchet 2001, Wyser et al. 2007), and Greenland topography (Box & Rinke 2003) for Arctic simulations.

Their higher resolution when compared to GCMs allows for fine-scale details to be added upon the driving large-scale flow. Despite the fact that RCMs are constrained by lateral boundary conditions (LBCs), recent studies have shown that RCMs also exhibit internal variability. This variability is usually understood as the capacity of the model to produce different solutions for the same set of LBCs and appears to vary as a function of season, domain size, and geographical location (e.g., CAYA & BINER 2004).

Careful design of an RCM domain and specification of the Lateral Boundary Conditions (LBCs) from analysed fields allows an RCM to be constrained to follow the observed large-scale atmospheric evolution, while still permitting local interactions between parameterizations and the model's resolved dynamics. Furthermore, the spatial resolution of the model and therefore the scales classified as unresolved are well defined in an RCM. Careful design of an RCM grid can allow simulated variables to be confidentially evaluated against localised observations for a time-limited period, as is often the case with intensive observation campaigns. Comparisons can then be made over a common thermodynamic phase space, with less chance that dynamical mismatches in space or time render the time-limited comparison meaningless.

The Arctic Regional Climate Model Intercomparison Project (ARCMIP, CURRY & LYNCH 2002) was developed to assess and document the performance of atmospheric RCMs over the Arctic. The first ARCMIP experiment was designed to capitalise on the SHEBA observation campaign (UTTAL et al. 2002), occurring in the western Arctic between September 1997 and October 1998. The ARCMIP model domain was designed with the SHEBA observation camp at its centre (RINKE et al. 2006). The large amount of cloud and radiation observations taken at SHEBA offers the potential to evaluate RCM cloud–radiation simulations over the Arctic and to utilise the observed data in further improving deficiencies identified in the RCM parameterization with respect to surface albedo and clouds.

Clouds play a key role in regulating the surface energy budget of the Arctic Ocean (CURRY et al. 1995) and are, therefore, important indirect controls on the evolution of Arctic sea ice and the sea-ice/snow albedo feedback. Due to the unique conditions in the Arctic (e.g., extreme low temperatures and water vapour mixing ratios, highly reflective sea-ice/snow surfaces, low-level inversions and the absence of solar radiation for extended periods) the macrophysical and microphysical processes controlling cloud formation and cloud–radiation interactions are complex and unique. This has led to difficulties both in simulating Arctic cloud phenomena as well as observing clouds in the Arctic (WYSER et al. 2007, UTTAL et al. 2002). During winter the Arctic atmospheric boundary layer is extremely stable. As a result, deep surface-based temperature inversions are frequent. This situation leads to extensive low-level cloudiness with significant amounts of cloud-ice present.

In this paper we describe sensitivity experiments with atmospheric RCMs applied to the Arctic and in a single RCM application to Antarctica. The influence of atmosphere–ocean–sea-ice and atmosphere–land–soil interactions in coupled RCM simulations driven either by ERA or GCM boundary forcing data have been investigated for an Arctic setup. These deliver valuable information by improving the physical realism of the considered physical feedback processes. In one example we discuss the implementation of improved sea-ice albedo parameterization into a GCM, which results in global impacts. We discuss also the global impact of an interactive stratospheric chemistry scheme in the Arctic polar vortex. Finally we describe a two-way feedback approach allowing high resolution modelling of the Arctic within a global model system.

COUPLED AND UNCOUPLED REGIONAL CLIMATE MODEL SIMULATIONS

The polar areas of the ocean and atmosphere are distinguished from the rest of Earth's climate system by many special features of a regional or physical nature that signify key challenges for modelling and observations. They are characterized by very low atmospheric temperatures, marked seasonality, huge continental ice sheets, large oceanic areas, permanently or seasonally covered by sea ice, and massive and deep reaching permafrost layers.

Recent observations and climate modelling results (e.g., JOHANNESSEN et al. 2004) have highlighted the Arctic as a region of particular vulnerability to global climate change. The total Arctic warming since 1979 occurred with a magnitude of 0.46 ºC. It is two times larger than the global warming due to the polar amplification. Superimposed on this trend the Arctic climate system shows pronounced decadal-scale climate variability. The temperature changes in the Arctic are linked to natural modes of climate variability as the Arctic Oscillation (AO) and the Pacific Decadal Oscillation (PDO) as discussed by SERREZE & FRANCIS (2006). These trends in the large-scale teleconnection pattern are connected with trends in Arctic cyclones as shown by SERREZE et al. (1997) and SORTEBERG & KVINGEDAHL (2006). These global patterns can be influenced by regional feedbacks in the Arctic, as shown by DETHLOFF et al. (2006) and SOKOLOVA et al. (2007) for regional feedbacks connected with albedo effects.

Sea ice plays a prominent role in the Arctic climate system, because the presence of sea ice modifies the exchange of heat, moisture, and momentum between atmosphere and ocean, and therefore atmospheric and oceanic processes and circulations, which in turn have impact on the existence and spatial distribution of sea ice. The sea-ice–albedo feedback effect is an important factor in the amplification of climate change in the Arctic (e.g., CURRY et al. 1995) so that changes in Arctic sea ice have the potential to impact Arctic and global climate significantly. Hence, a realistic simulation of Arctic sea ice is one of the major challenges in coupled Arctic climate modelling.

Recent coupled model intercomparison studies have shown that different atmosphere–ocean–ice models (AOI models) produce quite different sea-ice thickness and extent already in their present-day climate. Therefore, it is not surprising that projections of the 21st century ice extent by these models differ considerably from each other and are strongly dependent on the models' simulations of present-day ice extent (WALSH & TIMLIN 2003, HOLLAND & BITZ 2003). The development of regional atmosphere only models applied to the Arctic started with the works of WALSH et al. (1993), LYNCH et al. (1995) and DETHLOFF et al. (1996). MASLANIK et al. (2000), RINKE et al. (2003) and MIKOLAJEWICZ et al. (2005) applied coupled regional models to understand the feedbacks in the Arctic climate system.

ARCMIP simulations for the SHEBA year

The Arctic regional climate model intercomparison project ARCMIP focused on coordinated simulations by different Arctic RCMs and their evaluation using observations from satellites and field measurements. The combination of model intercomparison and evaluation using observations allows to assess strengths and weaknesses of model structures, numerics and parameterizations. The simulation experiments are carefully designed so that each of the models is operating under the same external constraints (e.g., domain, boundary conditions). The ARCMIP experiment 1 has been conducted for the 1997/1998 period of Surface Heat Budget of the Arctic Ocean Project (SHEBA), which included extensive field observations and accompanying satellite analyses.

All RCMs used a common set of lateral boundary conditions (LBC) derived from ECMWF (European Centre for Medium-Range Weather Forecasts) operational analyses. Sea-ice concentrations were specified using six-hourly SSM/I satellite data (COMISO 2002), while prescribed sea surface temperatures (SST) and sea-ice temperatures were derived from six-hourly satellite observations, using the NOAA-AVHRR (Advanced Very High Resolution Radiometer) instrument (KEY 2001). Snow accumulation and melting is computed by the RCMs, implying potential differences in the surface albedo between the various models. The surface temperatures over land and glaciers are not prescribed, but calculated individually by each model, using their own energy balance calculations. The models differ in the vertical resolution as well as in the treatments of dynamics and physical parameterizations. TJERNSTRÖM et al. (2005), RINKE et al. (2006) and WYSER et al. (2007) discussed the results of this first intercomparison experiment.

Simulations of eight different Arctic RCMs (ARCSyM, COAMPS, CRCM, HIRHAM, RegCM, PolarMM5, RCA and REMO) have been performed for the SHEBA period as explained in Table 1. Each of the models employed the same domain covering the Beaufort Sea (~70x55 grid points), the same horizontal resolution of 50 km, and the same atmospheric lateral boundary (ECMWF analyses) and the same ocean–sea-ice lower boundary forcings (AVHRR, SSM/I). Figure 1a shows the geography of the integration domain for the ARCMIP experiment together with the SHEBA trajectory and the pan-Arctic integration domain used in atmosphere only and coupled regional model simulations. This figure also covers the bigger pan-Arctic integration area used in the atmosphere only and regionally coupled model simulations described below.

Compared with the SHEBA observations, the modelled near surface variables (e.g., surface pressure, temperature, wind, radiation, etc.) agree well with the observations. The model ensemble mean bias in net radiation is -10 W m^{-2} and less than 1 m s^{-1} in wind. Although the mean turbulent heat flux bias is also small, the models differ strongly from each other and reveal some common bias features compared to ECMWF analyses. They share a common large-scale flow bias in all seasons (an underestimation of the geopotential height by the models) and a common seasonal bias in temperature and humidity profile (models are colder in lower levels in the transition periods and warmer elsewhere, relatively dry in the near surface layers and wet in the free troposphere) compared to ECMWF analyses. Even using a very constrained experimental design (small integration domain, specified lower boundary condition for ocean and sea ice) and specified "perfect" horizontal boundary conditions from data analyses, there is considerable scatter among the different RCMs.

Figure 1b shows the model ensemble of the 2-m temperature for summer and winter following RINKE et al. (2006). The largest across-model bias is found in the 2-m air temperature over land (up to 5 °C), which is connected to the bias in the surface radiation fluxes (up to 55 W m^{-2}), and in the cloud

Model	Responsible institution	Horizontal grid	Vertical grid	Vertical levels
ARCSyM	University of Colorado	Arakawa-B, 70×55 grid points Polar stereographic	Sigma, Top at 10 hPa	23
COAMPS	University of Stockholm	Arakawa-C, 70×55 grid points Polar stereographic	Sigma-z, Top at 34,800 m	30
CRCM	University of Quebec	Arakawa-C, 66×53 grid points Polar stereographic	Gal-Chen, Top at 29,042 m	29
HIRHAM	Alfred Wegener Institute (AWI)	Arakawa-C, 70×55 grid points Rotated latitude/longitude	Sigma-p, Top at 10 hPa	19
RegCM	Norwegian Meteorological Institute (met.no)	Arakawa-C, 66×53 grid points Rotated latitude/longitude	Sigma-p, Top at 10 hPa	19
PolarMM5	University of Colorado	Arakawa-B, 70×55 grid points Polar stereographic	Sigma, Top at 10 hPa	23
RCA	Swedish Meteorological and Hydrological Institute (SMHI)	Arakawa-C, 78×60 grid points Rotated latitude/longitude	Sigma-p, Top at 10 hPa	24
REMO	Max Planck Institute for Meteorology (MPI)	Arakawa-C, 70×55 grid points Rotated latitude/longitude	Sigma-p, Top at 10 hPa	20

Tab. 1: Horizontal and vertical grid information on the regional atmosphere models participating in the Arctic Regional Climate Model Intercomparison Project (ARCMIP).

Tab. 1: Angaben über die horizontalen und vertikalen Gitter der regionalen Atmosphärenmodelle, die am „Arctic Regional Climate Model Intercomparison Project" (ARCMIP) beteiligt sind.

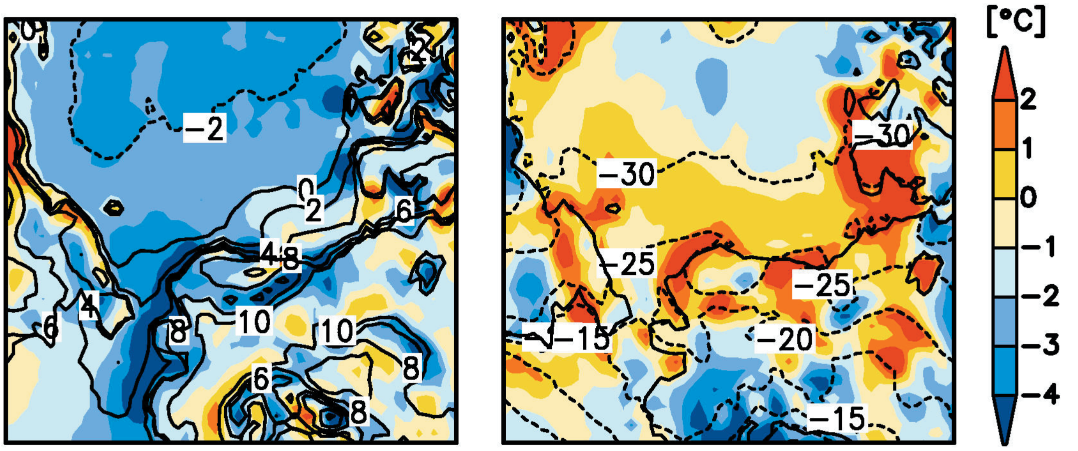

Fig. 1b: Mean 2-m air temperature [°C] in summer (= left) and in winter (= right) of the eight-mod-el ensemble from the Arctic Regional Climate Model Intercomparison Project (= isolines) and the respective bias of the ensemble mean compared to ERA-40 data (= colour fields). Tempera-tures are shown for the ARCMIP integration domain from Figure 1a.

Abb. 1b: Mittlere 2 m-Lufttemperatur [°C] im Sommer (links) und im Winter (rechts) des 8-Modell-Ensembles vom „Arctic Regional Climate Model Intercomparison Project" (= Isolinien) und die jeweilige Abweichung des Ensemblemittels gegenüber ERA-40-Daten (farbige Flächen). Die Temperaturen sind für das ARCMIP-Integrationsgebiet aus Abbildung 1a dargestellt.

cover (5-30 %), not shown. This is not surprising given the very complex and individually different land-surface and radiation-cloud schemes within the models. The quantified scatter between the individual models highlights the magnitude and seasonal dependency of the disagreement and unreliability for current Arctic regional climate simulations. The mentioned scatter is similar to the model scatter of climate change scenarios. The stronger model deviations in winter are due to differences in the simulation of meso-scale cyclones, as discussed by Rinke et al. (2006).

Since most of the physical parameterizations are adapted for global and midlatitude climate simulations, they are not always sufficient for the specific Arctic climate conditions, for example, for the vertical diffusion in a shallow stable boundary layer, discussed below. Several efforts have been done to develop improved process descriptions for Arctic climate simulations. A new snow albedo scheme was developed with a surface temperature dependent scheme, which is different for forested (linear dependency) and non-forested (polynomial approach) areas. A new sea ice albedo with three different surface types (snow covered ice, bare sea ice, melt ponds) and a surface temperature dependent scheme with a linear dependency was developed by Køltzow et al. (2003). By implementing this scheme into the HIRHAM model for the pan-Arctic domain it was shown that the gross features of the annual surface albedo cycle are reproduced by such a surface temperature dependent scheme. A polynomial temperature dependency of snow albedo improves HIRHAM simulations in spring compared to the old linear temperature dependency and improves especially the surface air temperature in spring and autumn. This new scheme improves the mean sea level pressure in spring and autumn, but decreases mean sea-level pressure (MSLP) skill in mid-summer compared to ERA40. HIRHAM is highly sensitive to the surface albedo for the large Arctic simulation area.

Future simulations made within the ARCMIP project will evaluate improvements made to parameterizations in the light of these findings and subsequently test these improvements in coupled Arctic RCMs, where sea ice and SSTs are free to respond to the simulated surface radiation. The Arctic environment, with its semi-permanent sea ice, sets up unique atmospheric boundary-layer conditions. The annual cycle is very large, while the diurnal cycle, which influences the boundary-layer structure at many midlatitude locations, is often absent. During Arctic winter, the snow-covered ice insulates the atmosphere from the relatively warm ocean. Combined with the absence of solar warming, strong long-wave surface cooling facilitates the formation of long-lasting surface inversions with strongly stable conditions.

Importance of the Arctic planetary boundary layer parameterizations

The Arctic planetary boundary layer (PBL) is stably stratified about 75 % of the time (Persson et al. 2002) and turbulence in very stable conditions is generally poorly understood (Mahrt 1998). The longevity of the stable conditions makes the interplay between gravity waves and turbulence relatively more important (Zilitinkevich 2002). During summer the ice melts, which efficiently regulates the low-level atmospheric temperature. Additional energy input melts the snow and ice rather than heating the surface, while energy loss results in the freezing of water rather than the cooling of the surface. Long periods of stable PBL conditions in winter are interspersed with periods of near-neutral conditions, forced by long-wave radiation (Persson et al. 2002) directly related to boundary-layer clouds, also a known problem for models.

Dethloff et al. (2001) investigated the influence of different planetary boundary layer (PBL) parameterizations on the Arctic circulation in experiments with the regional atmospheric climate model HIRHAM. The first experiment was set up with the PBL parameterization of the atmospheric circulation model ECHAM3, including the Monin-Obukhov similarity theory in the surface layer and a mixing length approach (labelled with ECHAM3_MO). The second experiment used the ECHAM3 parameterization with the Rossby-number similarity theory for the whole PBL, connecting external parameters with turbulent fluxes and with universal functions determined on the basis of Arctic data (labelled with ECHAM3_RO). The third experiment was carried out using the ECHAM4 parameterizations with a turbulent kinetic energy (TKE) closure (labelled with ECHAM4).

The HIRHAM model has been applied on the pan-Arctic domain for a wide range of applications (e.g., DETHLOFF et al. 2001, RINKE et al. 2004, DETHLOFF et al. 2004). The vertical discretization consists of 19 irregularly spaced levels. HIRHAM contains the physical parameterization package of the general circulation model ECHAM4, which includes radiation, cumulus convection, planetary boundary layer and land surface processes, and gravity wave drag. A time step of 5 min is used. The model is forced at the lateral boundaries by temperature, wind, humidity, and surface pressure (updated every six hours). At the lower boundary over land grid points, the soil temperatures and water are initialized according to climatology and afterward are calculated every time step using the energy and water budget equations. At the ocean lower boundary the model is forced by SST, sea-ice fraction and thickness (updated daily). The sea-ice surface temperature is calculated prognostically via a heat balance equation linearized in both temperature and time. Sea ice is treated by a scheme taking into account fraction and thickness of sea ice. Sea ice affects the atmospheric simulation in the model via two main processes: the atmosphere–ocean heat exchange and the albedo effect. In the boundary layer scheme, the effects of fractional sea-ice cover on the roughness length and on turbulent heat fluxes are included. In the radiation scheme, a grid cell-averaged surface albedo is used. The ice albedo is surface temperature dependent and accounts for meltwater ponds on ice near the melting ponds. The prescribed sea-ice thickness influences the thermal conduction through the ice.

The near surface temperature, the large-scale fields of geopotential and horizontal wind simulated in the sensitivity experiments by DETHLOFF et al. (2001) are satisfactorily described by all three schemes, but strong regional differences occur. The results show sensitivity to the type of the turbulence exchange scheme used. The comparison with ECMWF analyses and with radiosonde data reveals that during January the ECHAM3 scheme with Rossby-number similarity theory more successfully simulates the cold and stable PBL over land surfaces, whereas over the open ocean ECHAM3 parameterization with Monin-Obukhov similarity works better. The ECHAM3 scheme with Rossby-number similarity theory delivers a better adapted vertical heat exchange under stable Arctic conditions and reduces the cold bias at the surface. The monthly mean surface turbulent heat flux distribution strongly depends on the use of different PBL parameterizations and leads to different Arctic climate structures throughout the atmosphere with the strongest changes at the ice edge for January.

Figure 2 presents the mean sea-level pressure (MSLP) and 10 m wind speed distribution over the whole Arctic for July 1990 from the three experiments. The ECHAM4 version simulates a low-pressure area over the central Arctic, which extends more to the Siberian region. The low over Siberia, which appeared in the ECMWF analyses, disappears and the high over Greenland seems more developed. The monthly mean circulation structures produced by ECHAM3_RO are characterized by a deeper low over the Central Arctic. The best agreement with the ECMWF analyses during summer has been obtained with the ECHAM4 scheme using a TKE closure. For all PBL schemes the lowest temperatures occur over the Arctic Ocean. These simulations showed the importance of different PBL schemes not only for the local vertical temperature structures,

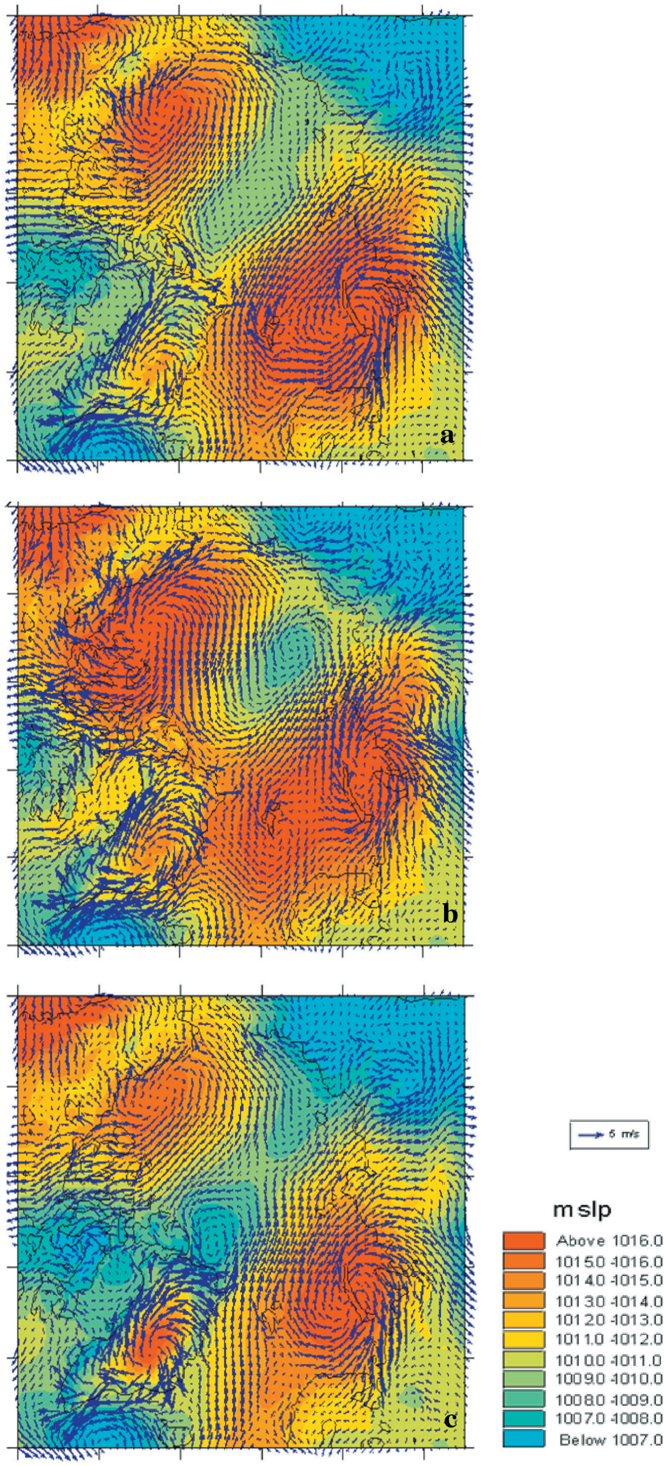

Fig. 2: Sea level pressure [hPa] and 10-m wind [m s^{-1}] in July 1990 over the pan-Arctic integration domain from HIRHAM simulations with different turbulent PBL closure schemes but identical lower and lateral boundary forcing. (Top) = ECHAM3 parameterizations with Monin-Obukhov similarity theory, (middle) = ECHAM3 parameterizations with Rossby-number similarity theory, (bottom) = ECHAM4 parameterizations with turbulent kinetic energy closure.

Abb. 2: Luftdruck in Meeresniveau [hPa] und 10m-Wind [m s^{-1}] im Juli 1990 über dem gesamtarktischen Integrationsgebiet aus HIRHAM-Simulationen mit unterschiedlicher Turbulenzschließung in der planetaren Grenzschicht, aber identischem unteren und seitlichen Randantrieb. (Oben) = ECHAM3-Parametrisierungen mit Monin-Obukhov-Ähnlichkeitstheorie, (Mitte) = ECHAM3-Parametrisierungen mit Rossby-Zahl-Ähnlichkeitstheorie, (unten) = ECHAM4-Parametrisierungen mit Schließung über die turbulente kinetische Energie.

but also for remote impacts on the atmospheric circulation over the Arctic Ocean.

TJERNSTRÖM et al. (2005) showed for the ARCMIP simulations, that some of the errors in the boundary layer have their roots elsewhere in the model. Most of the systematic errors are different in the lowest kilometre than aloft, but they seldom approach zero with altitude, despite applying the same lateral boundary conditions to all models. These results lead to the conclusion that there are uncertainties in current modelling of Arctic climate processes that must be reduced by improving important process descriptions in climate models.

Many physical processes in climate models are not resolved and therefore need to be parameterised. Development of parameterizations always involves an empirical component. Detailed process observations in the Arctic are, however, sparse and consequently the ensemble of observations forming the empirical basis for the development of reliable parameterizations may therefore be inadequate. It is important to develop, test and evaluate such schemes using in situ measurements from the Arctic. Until quite recently, this was difficult due to the lack of adequate data representing a reasonable ensemble of Arctic conditions. This situation is improving, with new experiments in the Arctic, e.g., the SHEBA (PEROVICH et al. 1999) experiment and AOE-2001 (LECK et al. 2004).

Coupled regional atmosphere–ocean–sea-ice model of the Arctic climate system

The improved parameterizations need a coupled Arctic RCM test environment, where sea ice and SSTs are free to respond to the simulated surface radiation. A coupled regional atmosphere–ocean–sea-ice model of the Arctic climate system has therefore been developed at AWI over the past years (RINKE et al. 2003, DORN et al. 2007, 2008). The coupled model consists of the atmosphere model HIRHAM with horizontal resolution of 0.5° and 19 vertical levels, covering the pan-Arctic integration domain and the ocean–ice model NAOSIM with horizontal resolution of 0.25° and 30 vertical levels. NAOSIM is based on MOM-2 and uses elastic-viscous-plastic sea-ice rheology and zero-layer thermodynamics for sea ice and snow. A series of sensitivity experiments has been carried out for the period from May 1989 to December 1999, in which the coupled regional model was driven by ERA-40 at HIRHAM's lateral boundaries and also at HIRHAM's lower and NAOSIM's upper boundary points that lie outside of the overlap area of the two model domains. In order to analyse the impact of the initial sea-ice conditions, an experiment (labelled as init-ice) was performed in which the initial ice thickness was uniformly set to 1 m in all grid cells with ice cover greater than 50 %, while all other grid cells were initialized with open water. In all other experiments, the initial ocean and sea-ice fields were taken from a stable run of the stand-alone ocean–ice model.

Figure 3 shows simulated monthly means of sea-ice volume and sea-ice extent, the latter in comparison with SSM/I satellite derived data using the NASA Team algorithm (CAVALIERI et al. 1990, updated 2004). It is quite obvious that the sea-ice volume is far from a steady state at the beginning in all coupled model experiments, even if initialized with sea-ice fields from a stable run of NAOSIM (control and newalb experiments). However, all simulations arrive at a quasi-stationary cyclic state of equilibrium after about 6-10 years, and this equilibrium is only little affected by the initial sea-ice state. The coupled model's state of equilibrium depends significantly on the rate of increase in ice concentration, but it is also significantly affected by the parameterization of the sea-ice albedo as seen in an experiment (labelled as newalb in Fig. 3) which uses a new sea-ice albedo scheme adapted from version 2 of KØLTZOW et al. (2003), described above.

A rough comparison with available ice thickness observations, for instance with the climatology of LAXON et al. (2003), shows that the control experiment (Fig. 3) is closest to these observations, while the albedo experiment (newalb) clearly underestimates the ice thicknesses. The corresponding sea-ice extent of the control and albedo experiments (Fig. 3) reveals that both simulations overestimate summer ice extent during the first years, but at least the control experiment agrees quite well with the observations after some years, while the albedo experiment then tends to underestimate the summer ice extent considerably. A common result of the experiments is that summer ice extent is significantly correlated with the ice volume at the beginning of the melting period (ensemble correlation coefficient of 0.92 between ice volume in April and ice extent in September). On the other hand, the model generally overestimates the sea-ice extent during winter, and none of the experiments has been able to reduce this shortcoming substantially.

An important feature of the new albedo scheme is that it decreases the ice albedo in most instances, particularly for melting conditions when snow has already disappeared. As a result, the energy input into the ocean–ice system is increased by the new scheme, leading to quicker decay of sea ice during summer and accordingly to reduced ice volume at the end of the summer. In addition, there is not only an indirect influence on summer sea ice by the changed ice volume but also a direct modification of sea ice and atmospheric conditions due to the albedo-related change of the radiative fluxes.

Figure 4 shows the SSM/I satellite derived and modelled sea-ice concentration in September 1998. The experiments demonstrate the strong effects of an unrealistic ice thickness distribution on summer ice extent and concentration: If the sea ice is too thin at the beginning of the melting period, the ice cover is quicker to open with the result of stronger ice retreat and underestimation of sea-ice concentration throughout the Arctic. In contrast, too thick sea ice results in effects exactly the opposite to the above. The control experiment, which ice thicknesses are closest to reality, also shows the best agreement in ice extent and concentration.

Although the experiment with the new albedo scheme shows quasi-realistic sea-ice retreat in the Beaufort Sea and also in the Barents and Kara seas, there are considerably larger areas of open water in the Laptev and East Siberian seas. This underestimation of sea ice is associated with differences in the atmospheric circulation during the previous summer months (Fig. 5). In contrast to observations and the other model experiments, the albedo experiment shows a pronounced cyclone over the Laptev Sea which provides an atmospheric flow for

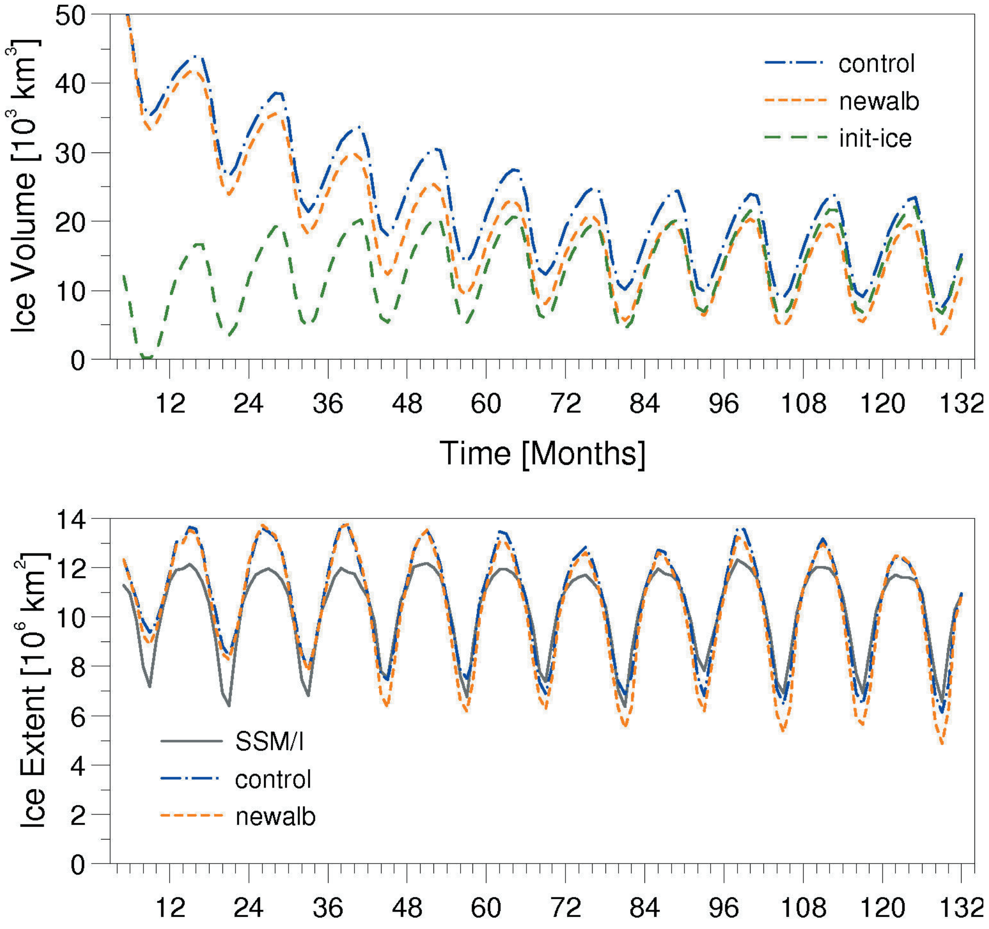

Fig. 3: Simulated monthly means of sea-ice volume (top) and sea-ice extent (bottom) within the pan-Arctic model domain from May 1989 (month 5) to December 1999 (month 132). The sea-ice extent is here defined as the area of all grid cells with at least 15 % sea-ice concentration. For comparison, the SSM/I satellite derived sea-ice extent (solid grey line) was calculated for the same domain. The model simulations with HIRHAM–NAOSIM were carried out with standard ice albedo scheme and standard ice initialization (control = blue lines), with new ice albedo scheme and standard ice initialization (newalb = or-ange lines), and with standard ice albedo scheme and initialization with uniform 1 m ice thickness (init-ice = green line).

Abb. 3: Simulierte Monatsmittel des Meereisvolumens (oben) und der Meereisausdehnung (unten) innerhalb des gesamtarktischen Modellgebiets von Mai 1989 (Monat 5) bis Dezember 1999 (Monat 132). Die Meereisausdehnung ist hier als die Fläche aller Gitterzellen mit mindestens 15 % Meereiskonzentration definiert. Zum Vergleich wurde die aus SSM/I-Satellitendaten abgeleitete Meereisausdehnung (graue Linie) für das gleiche Gebiet berechnet. Die Modellsimulationen mit HIRHAM–NAOSIM wurden mit dem Standard-Eisalbedo-Schema und der Standard-Eisinitialisierung (control = blaue Linien), mit dem neuen Eisalbedo-Schema und der Standard-Eisinitialisierung (newalb = orange Linien) und mit dem Standard-Eisalbedo-Schema und Initialisierung mit einheitlich 1 m dickem Eis (init-ice = grüne Linie) durchgeführt.

drifting ice away from the East Siberian seas towards the central Arctic Ocean and Kara Sea. The redistribution of ice mass within the Arctic leads to a situation in which thermodynamic loss of ice is regionally either intensified by dynamic ice loss or partly compensated by increased influx of ice.

In order to achieve a realistic regional distribution of sea ice in late summer, it is also required that the coupled model reproduces the observed atmospheric circulation during the preceding summer months. But in contrast to the clear response of the sea-ice cover to the atmospheric circulation, the atmospheric response to incorrect sea-ice cover is not that definite. Unrealistic sea-ice cover, as a result of incorrect thermodynamic ice loss, may favour model deviations in atmospheric circulation, but these deviations can clearly differ in their strength, probably in consequence of regional feedbacks. Owing to the variety of processes involved in such regional feedbacks, it is hard to distinguish between cause and effect of model deviations in a coupled model system without systematic sensitivity experiments. A sample of such experiments have been presented here and in the work of DORN et al. (2007), but a couple of further experiments, especially with respect to the cloud scheme and the treatment of snow and ice melt, are required to assess the importance of individual processes for the simulation of Arctic sea ice and to develop improved parameterizations for these processes.

DORN et al. (2008) showed by means of a 21-year simulation of a coupled regional pan-Arctic atmosphere–ocean–ice model for the 1980s and 1990s and comparison of the model results with SSM/I satellite-derived sea-ice concentrations, the patterns of maximum amplitude of interannual variability of the Arctic summer sea-ice cover are revealed. They are shown to concentrate beyond an area enclosed by an isopleth of barotropic planetary potential vorticity that marks the edge of the cyclonic rim current around the deep inner Arctic basin. It is argued that the propagation of the interannual variability signal farther into the inner Arctic basin is hindered by the dynamic isolation of upper Arctic Ocean and the high summer cloudiness usually appearing in the central Arctic. The thinning of the Arctic sea-ice cover in recent years is likely to be jointly responsible for its exceptionally strong decrease in summer 2007 when sea-ice decline was favoured by anomalously high atmospheric pressure over the western Arctic Ocean, which can be regarded as a typical feature for years with low sea-ice extent. In addition, unusually low cloud cover appeared in summer 2007, which led to substantial warming of the upper ocean. It is hypothesized that the coincidence of several favourable factors for low sea-ice extent is responsible for this extreme event. Owing to the important role of internal climate variability in the recent decline of sea ice, a temporal return to previous conditions or stabilization at the current level can not be excluded just as further decline.

Coupled atmosphere–permafrost model of the Arctic climate system

Beside the Arctic sea-ice cover also the polar land surface is known to be an important part of the climate model. It controls

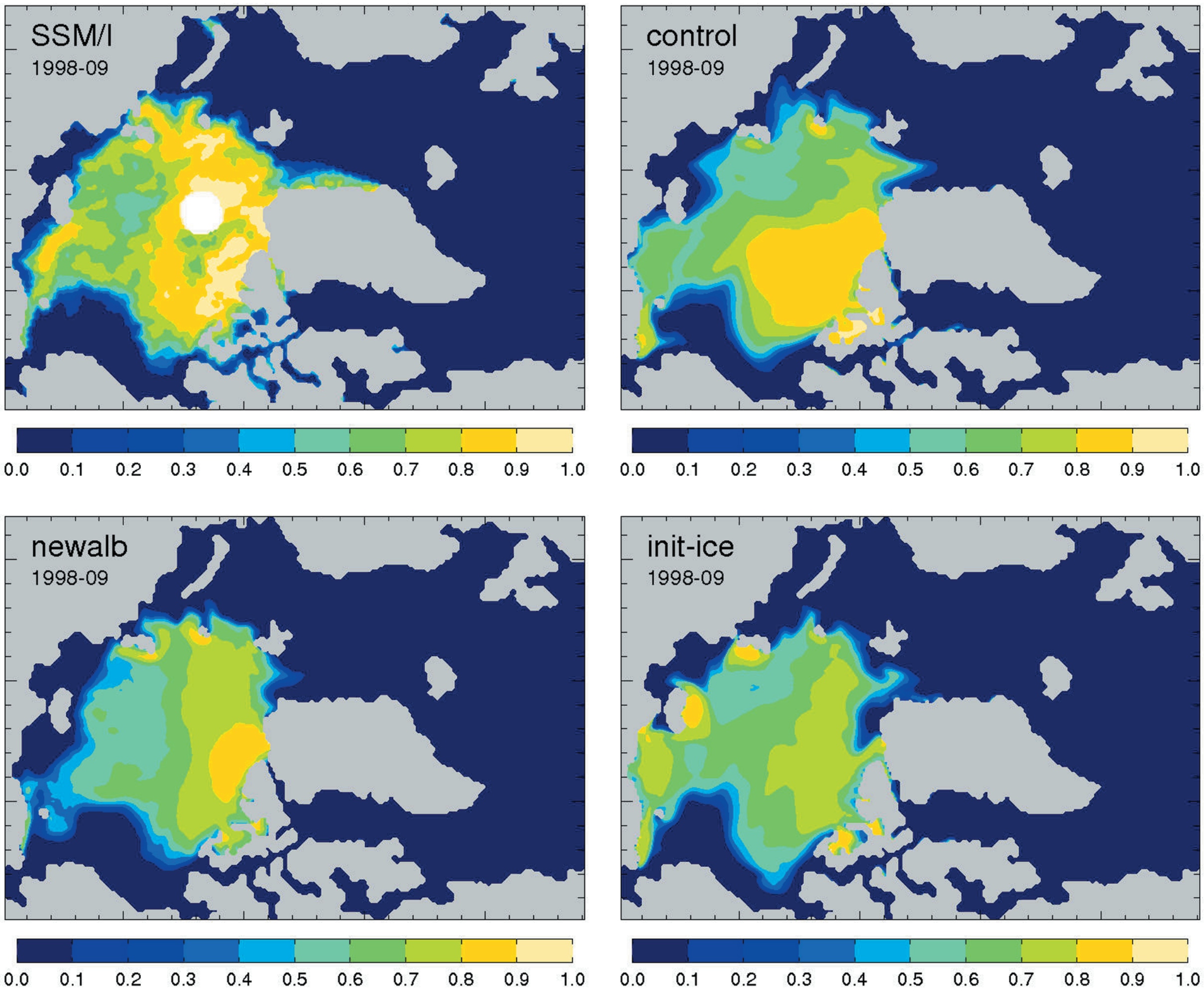

Fig. 4: Sea-ice concentration in September 1998 from SSM/I satellite derived data (= top left) and three simulations of the coupled regional model HIRHAM–NAOSIM with standard ice albedo scheme and standard ice initialization (control = top right), with new ice albedo scheme and standard ice initialization (newalb = bottom left), and with standard ice albedo scheme and initialization with uniform 1 m ice thickness (init-ice = bottom right).

Abb. 4: Meereiskonzentration im September 1998 abgeleitet aus SSM/I-Satellitendaten (= oben links) und drei Simulationen des gekoppelten regionalen Models HIRHAM–NAOSIM mit Standard-Eisalbedo-Schema und Standard-Eisinitialisierung (control = oben rechts), mit neuem Eisalbedo-Schema und der Standard-Eisinitialisierung (newalb = unten links) und mit Standard-Eisalbedo-Schema und Initialisierung mit einheitlich 1 m dickem Eis (init-ice = unten rechts).

the surface radiative heat budget, which partly depends on the optical properties of the land cover (i.e., emissivity, reflectivity). Partitioning of the surface available energy into sensible and latent heat and available water into evaporation and runoff are also performed by the land surface. BETTS (2000) showed that the forestation has a large impact on surface albedo over regions with long-lasting snow cover such as east Siberia. Such regional changes in surface albedo can have a global impact on the atmospheric circulation (DETHLOFF et al. 2006).

There exist close interactions between the atmosphere and the land surface. Therefore, changes in the land surface processes affect the atmospheric circulation and *vice versa.* About one quarter of the land surface in the Northern Hemisphere is permafrost region (ZHANG et al. 2000). However, the interactions between the atmosphere and Arctic land surfaces or permafrost are still poorly understood as they are very complex. Snow cover, vegetation type, soil type, soil moisture content, phase changes of soil moisture and planetary boundary layer structure above the surface are all involved into these interactions (VITERBO et al. 1999).

Most of the global models and Arctic regional climate models (RCMs) include simple land surface models (LSMs), and neglect processes like seasonal thawing/freezing of active layer, subsurface drainage of soil moisture, and snow processes like aging. However, such processes are particularly relevant for an Arctic domain. It has been shown that the inclusion of soil moisture freezing/thawing processes improves the boreal soil and surface air temperature simulations (BONAN 1998, LUO et al. 2003) and can exert a significant impact on projected 2 x CO_2 climate. Because of the potential warming of permafrost temperatures and increase of active layer depth by the mid of the 21st century, the land surface/soil processes and their linkages to the atmosphere must be better understood and taken into account in the Arctic RCMs to get more reliable estimates of future climate changes. It can be assumed that different land surface schemes can have significant impacts on the future projection of Arctic climate.

The limited amount of long-term soil temperature measurements complicates the systematic validation of pan-Arctic soil temperature in a high-resolution RCM. For Russia, such long-term records are available (BARRY et al. 2001) and used in this

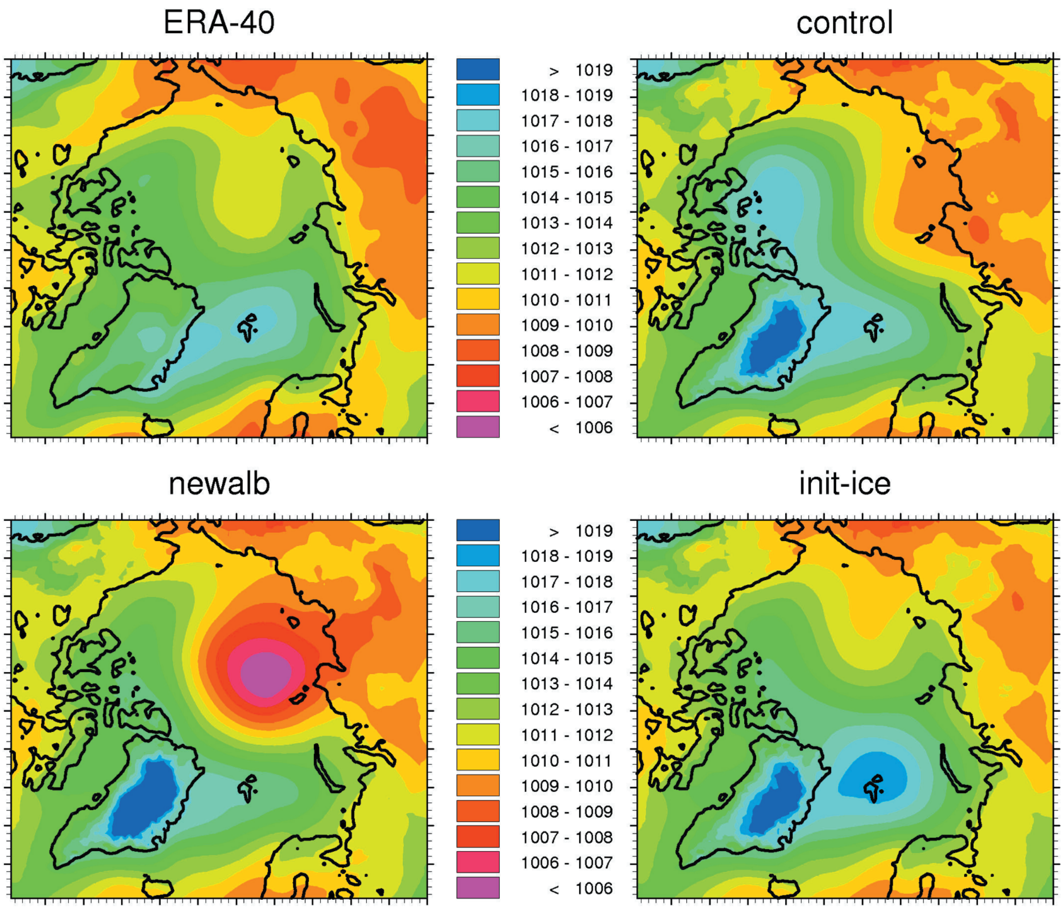

Fig. 5: Mean sea level pressure [hPa] in summer 1998 (June to September) from ERA-40 data (= top left) and the same model simulations as in Figure 4; control = top right; newalb = bottom left; init-ice = bottom right.

Abb. 5: Mittlerer Luftdruck in Meeresniveau [hPa] im Sommer 1998 (Juni bis September) aus ERA-40-Daten (= oben links) und denselben Modellsimulationen wie in Abbildung 4; control = oben rechts; newalb = unten links; init-ice = unten rechts

study. With this, the performance of a simplified LSM (Roeckner et al. 1996) and a complex LSM (Bonan 1996) is investigated within an Arctic RCM. This examination is motivated by, and aims to shed light on, a number of questions. Can a simple LSM simulate realistically the evolution of the soil temperature profile in the Arctic? What is the impact and added value of an advanced LSM, which takes key Arctic soil processes like freezing/thawing into account? Is the impact of a different LSM in an RCM limited to the local-regional scales or does it have a broader impact on the Arctic circulation?

A new land-surface model (LSM) from NCAR has been coupled with HIRHAM (HIR-LSM) in the Arctic permafrost region taking into account six soil layers as described by Saha et al. (2006, 2006a). The new coupled atmosphere-soil model has reduced the cold winter bias in the soil and improved also the summer 2-m air temperature. The new land surface scheme has a significant influence on the future projection of the Arctic temperature, precipitation and mean sea level pressure. The temperature differences between the HIRHAM coupled LSM and the old HIRHAM4 projections for the time period (2024-2029) minus (1990-1995) have been computed using the IPCC B2 scenario of ECHO-G.

Global B2 scenario simulations show for the last three decades of the 21st century (2071-2100), a change of 2.2 K – with a range of 0.9 to 3.4 K between the nine models used by IPCC – in globally averaged surface air temperature relative to the period 1961–1990. However, the models differ significantly in the simulated temperature response in the Arctic, not only in the magnitude but also in regional aspects of the projected temperature change. A model with high horizontal resolution will be very useful to find out the regional aspects of Arctic climate changes in the context of global warming. A dynamical downscaling of a B2 scenario simulation of the coupled atmosphere–ocean model ECHO–G (ECHAM4-HOPE–G) was done with the regional atmospheric model HIRHAM over a pan-Arctic domain at a horizontal resolution of 50 x 50 km. Two six-year-long time slices (1990-1995 and 2024-2029) were chosen for the dynamical downscaling of this scenario with the HIRHAM as well as with the HIR-LSM (Fig. 6).

The regions of warming and cooling during 2024-2029 winter (DJF) compared to 1990–1995 winter are similar for both model HIRHAM and the model version HIR-LSM. With advanced vegetation and soil schemes, the HIR-LSM shows a deviation from HIRHAM in 2-m air temperature by about ±2 °C. In both scenario runs there is an enhanced warming over the eastern hemisphere and parts of northern America and a cooling over Alaska and Greenland. The difference plot shows that the impact of different soil schemes varies with a strong regional signature. The LSM reduces the anthropogenic warming over Siberia and enhances the warming over European Russia and northern Canada.

Both the HIRHAM and the HIR-LSM show a similar warming and cooling trend in 2-m air and 10-cm soil temperatures at high latitudes but the HIR-LSM shows a stronger soil warming than HIRHAM. The anthropogenic impact is amplified by the use of a more advanced land–soil scheme in the Arctic. This would have strong implications for the additional release of methane from permafrost areas.

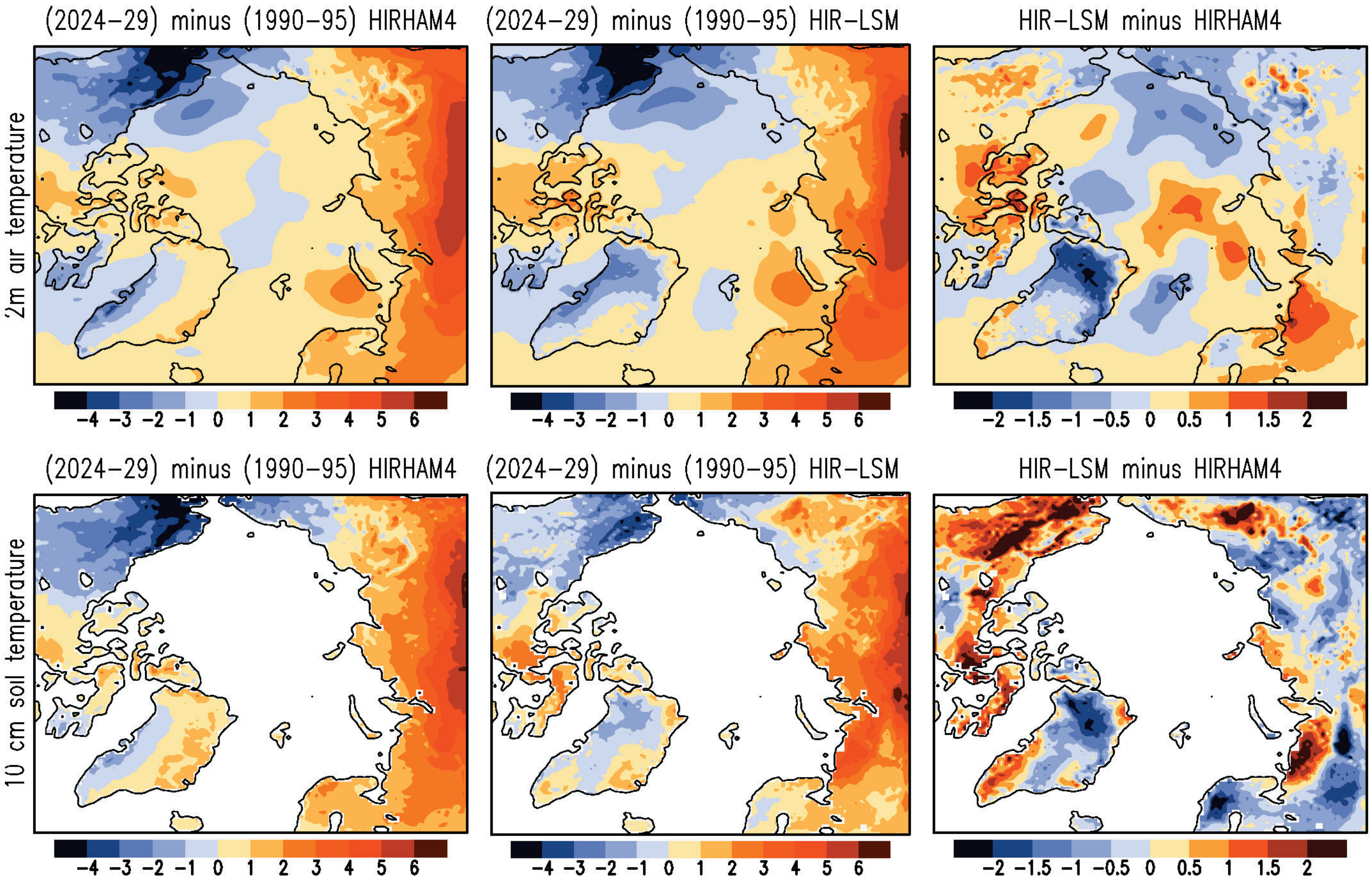

Fig. 6: Differences of mean 2-m air temperature [°C] (= top) and 10-cm soil temperature [°C] (= bottom) in winter (December to February) between time slice 2024-2029 and time slice 1990-1995 for the pan-Arctic integration domain. (Left) = HIRHAM simulation; (middle) = HIR-LSM simulation; (right) = difference between HIRHAM and HIR-LSM simulations.

Abb. 6: Differenz der mittleren 2-m Lufttemperatur [°C] (= oben) und der 10cm-Bodentemperatur [°C] (= unten) im Winter (Dezember bis Februar) zwischen Zeitscheibe 2024-2029 und Zeitscheibe 1990-1995 für das gesamtarktische Integrationsgebiet. (Links) = HIRHAM-Simulation; (Mitte) = HIR-LSM-Simulation; (rechts) = Differenz zwischen HIRHAM- und HIR-LSM-Simulation.

RINKE et al. (2008) incorporated a surface organic layer in the land-surface scheme of the Arctic regional climate model HIRHAM and discuss its implications for Arctic climate simulations. It is shown that this implementation modifies not only the ground thermal and hydrological regimes, but also strongly dynamically feeds back to the atmosphere. Changes in ground heat flux impact on atmospheric turbulent heat fluxes, which has consequences for the regional Arctic climate. The inclusion of the top organic layer reduces ground temperatures by 0.5 °C to 8 °C. Increased summer ground evaporation caused by the greater water holding capacity of the top organic layer causes a significant drop in 2-m air temperatures. Furthermore, climatologically important is the reduction of mean sea level pressure (SLP) over the Barents and Kara seas during winter, which would correct the well-known positive SLP bias over those regions in global climate models.

This result with its remote impacts clearly shows the need to improve the description of atmosphere–ocean–sea-ice and atmosphere–land–soil feedbacks in a coupled model setup and to upscale such results in a global model setup to reduce the existing model biases in polar regions.

Regional climate model simulations for the Antarctic

In a bi-polar approach beside the Arctic also the Antarctic plays a crucial role in the global climate system, since it is the principal region of radiative energy deficit, and is connected with the rest of the globe via meridional transports of heat, water and momentum. Further, a melting Antarctic ice sheet can affect atmospheric circulation, sea level, global ocean circulation, and the Earth's climate as a whole.

The current understanding of the Antarctic circulation and climate is still incomplete due to its complex interactions involving a variety of distinctive feedbacks. Processes that are not particularly well represented in the models are clouds, planetary boundary layer processes, and sea ice. The key features of Antarctic atmosphere are connected with the low surface temperature, strong surface inversion, and the persistent strong katabatic wind.

In terms of surface temperature changes across the continent in recent decades, there has been a warming of the Antarctic Peninsula and a small cooling around the coast of East Antarctica. The peninsula warming has been largest on the western side in winter and on the east during summer. The eastern warming has occurred largely because of more maritime air masses crossing the peninsula, as a result of the stronger westerlies through changes in the Southern Annular Mode (SAM). The warming is therefore, at least in part, a result of anthropogenic activity. The winter warming is believed to have occurred as a result of a decrease in sea-ice extent since the 1950s. This may be a result of increased cyclonicity over the Bellingshausen Sea in recent decades. The small cooling around the coast of East Antarctica is thought to be a result of changes in the SAM, which give a warming across the peninsula and cooling around East Antarctica.

Driven by boundary conditions from data analyses, RCMs tend to show smaller temperature and precipitation biases in the Antarctic compared to the GCMs (e.g., VAN LIPZIG et al. 2002, BROMWICH et al. 2004). However, temperature and precipitation biases are evident and thus our confidence in the 21st century projection over Antarctica is limited. Within the atmosphere, the interaction between clouds and radiation, the turbulent exchange between surface and air through the strong surface inversions, and the coupling of the atmosphere with the ocean–sea ice, they all modify the energy balance at the surface and therefore the surface temperature.

GLUSHAK (2008) applied the HIRHAM model on a circum-Antarctic domain. The model has been adapted to the extreme Antarctic conditions. Five additional vertical model layers have been included in the lowest 1000 m within the atmospheric planetary boundary layer to better resolve inversions, katabatic wind and the low-level wind jet. One long-term climate run (1958-1998) was carried out. The focus of the model validation was on the comparison with ERA-40 reanalyses. It has been shown that the principal climatological mean patterns of 2-m air temperature, mean sea level pressure, and 500-hPa geopotential and their interannual variability can be reproduced by the model well, although a cold model bias in summer is obvious. Also the comparison with selected station data shows the reasonable quality of the model simulations.

GLUSHAK (2008) computed the annual precipitation trends in HIRHAM simulations for the whole 40-year period (1958-1998) using the ERA-40 reanalyses. Because snow accumulation is critical in determining the evolution of the mass balance of the ice sheets, the precipitation amount is the most critical parameter for an accurate determination of accumulation. The accumulation term is the primary mass input to the Antarctic ice sheets, and is the net result of precipitation, sublimation/vapour deposition, drifting snow processes, melt and ice-mass flux divergence. Precipitation is dominant among these components and establishing its spatial and temporal variability is necessary to assess ice sheet surface mass balance. Precipitation is influenced to first order by the Antarctic topography. Most of the precipitation falls along the steep coastal margins and is caused by orographic lifting of relatively warm, moist air associated with the many transient, synoptic-scale cyclones that encircle the continent. The influence of synoptic activity decreases inward from the coast, and over the highest, coldest reaches of the continent the primary mode of precipitation is due to cooling of moist air just above the surface-based temperature inversion. This extremely cold air has little capacity to hold moisture, and thus the interior of the East Antarctic ice sheet is a polar desert. Figure 7 shows the annual precipitation trends from 1978-1998 for the ERA-40 data and the HIRHAM simulations. The location of the areas with negative precipitation trend is in agreement with a positive sea level pressure trend, indicating the strong connection between the cyclone tracks around the Antarctica and accumulation changes.

DAVIS et al. (2005) used satellite radar altimetry measurements from 1992-2003 to determine accumulation changes. These accumulation areas are well captured the HIRHAM simulations. The maxima and minima are in rather good agreement with the estimates by DAVIS et al. (2005) and are well captured by the HIRHAM simulations. During 1979-1998 the ERA-40 data show reduced accumulation trend while HIRHAM reveal a small area with 5-10 cm year^{-2} positive precipitation trend, which is captured by satellite measurements (8-10 cm year^{-2}).

POLAR CLIMATE PROCESSES AND GLOBAL LINKS

Teleconnection patterns and atmospheric circulation regimes

Recent observational studies of the Arctic region reveal significant changes in temperature, sea-ice distribution, precipitation, permafrost distribution and other climate variables (e.g., JOHANNESSEN et al. 2004). As discussed by SORTEBERG & KVINGEDAHL (2006), trends in the large-scale teleconnection patterns are connected with trends in Arctic cyclones. In order to attribute these changes to internally generated and externally forced climate variations, a general understanding of Arctic climate variability in the context of global climate variability is necessary. A basic concept for the understanding of climate variability is the concept of atmospheric circulation regimes. It is well known that atmospheric variability is

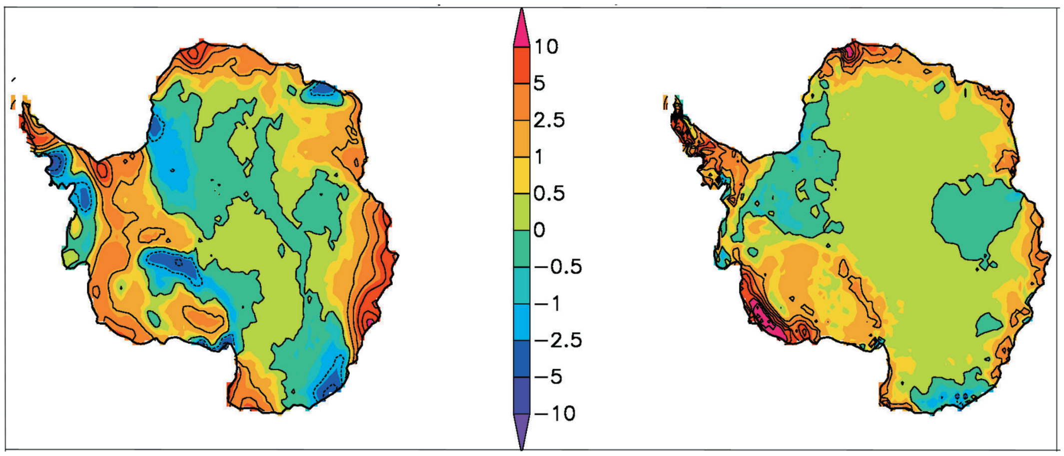

Fig. 7: Annual precipitation trend [cm year^{-2}] over Antarctica from 1978 to 1998 from ERA-40 data (= left) and HIRHAM simulations (= right).

Abb. 7: Jährlicher Niederschlagstrend [cm year^{-2}] über Antarktika von 1978 bis 1998 aus ERA-40-Daten (= links) und HIRHAM-Simulationen (= rechts).

characterised by a few preferred large-scale flow patterns which occur at fixed geographical regions. The concept of atmospheric circulation regimes connects these observations with atmospheric dynamics. In the framework of this concept, low-frequency climate variability can arise due to transitions between the distinct atmospheric regimes and is manifested, primarily, in terms of changes in the frequency of occurrence of the preferred circulation regimes (PALMER 1999). Analogy studies with simple nonlinear atmospheric models, data analyses, e.g., by CORTI et al. (1999), analyses of model runs with increased greenhouse gases (e.g., MONAHAN et al. 2000) and paleoclimatic simulations (CASTY et al. 2005) suggest, that response patterns of external forcing can in principle project onto natural variability modes, but the probability density of the preferred circulation regimes alters.

One method for the detection of preferred circulation patterns is the search for teleconnected regions in atmospheric data, by the method of empirical orthogonal function (EOF) analysis. As most studies, here we focus on the Northern Hemisphere (NH) winter months, when the atmosphere is dynamically most active and the global variability patterns have the largest influence on the Arctic climate. The application of the EOF method onto the extratropical NH fields of sea-level pressure (SLP) from NCEP-reanalyses from 1948-2007 reveals the most dominant surface patterns. These patterns are shown in Figure 8, in their positive phase. The most dominant variability pattern in the northern hemisphere (EOF1, explained variance 21.4 %) is the Arctic Oscillation (AO, THOMPSON & WALLACE 1998) representing an annular pattern with decreased SLP over the Arctic basin connected with increased SLP at mid-latitudes over the North Atlantic and North Pacific. This mode is strongly connected to the North Atlantic Oscillation (NAO). The NAO is the dominant mode of variability for the North Atlantic-European region and is mainly represented by a seesaw between Iceland and the Azores (HURRELL 1996).

The second variability pattern, explaining 13.2 % of total variance, is dominated by a North Pacific centre of action. Due to the similarity with the correlation pattern of the North Pacific Index (NP, TRENBERTH & HURRELL 1994) with SLP, it is referred as NP-related pattern. The dominant feature of the third pattern, which explains 9.3 % of SLP-variance, is a wave-train structure from the North Atlantic into the Arctic Ocean. The strongest pressure gradients are connected with rather strong meridional flow occur over the Barents Sea, thus this pattern is referred as Barents Sea (BS) pattern. Note, that this pattern is different from the Barents Sea Oscillation determined by SKEIE (2000) as EOF2 of the SLP field, because in the EOF analyses presented here a cosine correction has been applied to take into account correct area weighting.

During the positive phases of the NAO-AO (e.g., during the 1990s), lower SLP occurs in the whole Arctic, representing the

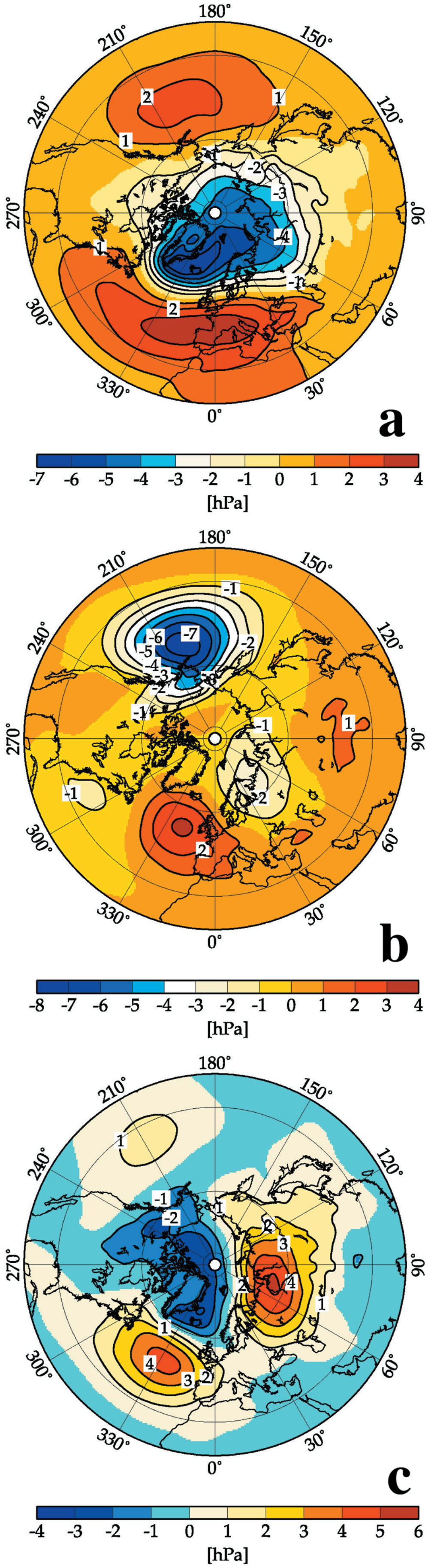

Fig. 8: The three leading variability patterns of the Northern Hemisphere; (top) = EOF 1; (middle) = EOF 2; (bottom) = EOF 3; obtained by an EOF analysis of the NCEP reanalysis monthly mean sea level pressure fields in the wintertime (December to February) from 1948–2007. The spatial area is confined to the extratropics from 20° N to 90° N.

Abb. 8: Die drei führenden Variabilitätsmuster der Nordhemisphäre; (oben) = EOF 1; (Mitte) = EOF 2; (unten) = EOF 3; ermittelt durch eine EOF-Analyse der monatsgemittelten Luftdruckfelder in Meeresniveau in den Wintermonaten (Dezember bis Februar) von 1948–2007 aus NCEP-Reanalyse-Daten. Das räumliche Gebiet beschränkt sich auf die Außertropen von 20° N bis 90° N.

typical atmospheric mass shift to mid-latitudes and subtropical regions. Northerly winds over Greenland and north-eastern Canada lead to negative temperature anomalies of surface air temperature (SAT) and sea surface temperature (SST). Related to the change of the mean circulation pattern, positive AO-NAO index is associated with a north-eastward shift in the Atlantic storm track with enhanced activity from Newfoundland to northern Europe and in the region of the Icelandic low. This is accompanied by fewer cyclones over the Barents and Kara seas (e.g., SERREZE et al. 1997).

DORN et al. (2003) showed that the effects of NAO regime changes on Arctic winter temperatures and precipitation are regionally significant over most of north-western Eurasia and parts of Greenland. In this regard, mean winter temperature variations of up to 6 K may occur over northern Europe. Precipitation and synoptic variability are also regionally modified by NAO regime changes with a stronger synoptic variability during positive NAO phases. The climate changes associated with the NAO are in some regions stronger than those attributed to enhanced greenhouse gases and aerosols. This result indicates that the projected global changes of the atmospheric composition and internal circulation changes are competing with each other in their importance for the Arctic climate evolution in the near future. The knowledge of the future AO-NAO trend on decadal time scales is vitally important for a regional assessment of climate scenarios for the Arctic.

The impact of the leading variability patterns on the Arctic circulation is not confined to the surface. Thus, the AO is not just the leading pattern at the surface, but shows a quasi-barotropic structure and is strongly coupled to the troposphere and the stratosphere (THOMPSON & WALLACE 1998) leading to a stronger and colder polar vortex (PV) during positive AO phase. The state of the PV does not only influence the propagation of planetary waves from the tropo- into the stratosphere, but also the migration of extreme anomalies from the stratosphere down to the troposphere. PERLWITZ & HARNIK (2003) suggested that zonal mean–planetary wave coupling dominates the downward interaction between strato- and troposphere during negative AO-phases, whereas reflection dominates this interaction during positive AO-phases. The relation of the more wave train-like variability patterns to the troposphere and stratosphere is much weaker and is dominated by baroclinic structures. How these patterns influence the vertical propagation of planetary waves and thus the flow in the tropo- and stratosphere as well as the troposphere-stratosphere coupling is a topic of ongoing research.

Global impacts of Arctic sea-ice albedo changes

All global models have their largest biases in the Arctic. Regional model systems with higher spatial and temporal resolutions and improved physics are more accurate as a result of forcing at the lateral and lower boundaries but their results are also uncertain because model intercomparison projects (MIP) have found striking inconsistencies among model outputs as discussed before. PROSHUTINSKY et al. (2008) identified a set of urgent improvements needed for different parameters and processes for both the regional and global Arctic models and gave recommendations for model improvements. The determination of uncertainty ranges would be of great importance for the reliability and robustness of regional climate change scenarios for the Arctic. In a sensitivity experiment we show the added value of upscaling a regionally important process, e.g., the ice albedo feedback process for the performance of global climate models in the polar regions.

Biases and across-model scatter are present e.g., in simulations of Arctic sea ice connected mainly with biases in the radiative forcing or in the parameterizations of surface melt and its influence on the absorption of shortwave radiation (FLATO et al. 2004). Main causes of the interannual variability of the sea-ice cover in the Arctic are the year-to-year variations in the atmospheric fields of wind and temperature due to the high sensitivity of the Arctic sea-ice cover to atmospheric forcing as discussed by ARFEUILLE et al. (2000). Sea ice introduces additional feedbacks into the coupled climate system, making climate naturally more variable in polar regions.

Surface albedo has long been recognized as one of the key surface parameters in climate models through its direct effect on the energy balance. By means of simulations with a global coupled AOGCM, Dethloff et al. (2006) investigated the influence of a more realistic sea-ice and snow albedo treatment changes on the energy balance and atmospheric circulation patterns. They found, that a more realistic sea-ice and snow albedo treatment changes the ice albedo feedback and the radiative exchange between ocean and the atmosphere. Sensitivity runs over 500 years with fixed solar constant (1365 W m^{-2}) and CO_2 (353 ppm) and the new ice- and snow albedo scheme for the Arctic of KØLTZOW et al. (2003) have been carried out by use of the state-of-the-art coupled global climate model ECHO-G. As shown by BENKEL & KØLTZOW (2006), the Arctic sea-ice coverage within ECHO-G is improved, especially the minimum sea-ice extent and area in summer. There is an Arctic cooling in winter and summer owing to the improved albedo parameterization similar to the results in the regional coupled climate models. Strongest global impacts occur during winter. Diagnostic studies have been carried out by computing the localized Eliassen-Palm fluxes which describe the interaction between the time-mean state and the transient eddies as discussed by SOKOLOVA (2006) and SOKOLOVA et al. (2007).

The localised Eliassen-Palm flux differences for the old snow and sea-ice albedo scheme from ECHAM4 and the new snow and sea-ice albedo scheme from KØLTZOW et al. (2003) for ECHO-G "New albedo minus Control" for eight years have been computed. Changes in the planetary wave trains and planetary wave pattern in high and mid-latitudes between tropics and Arctic over the Pacific and the Atlantic occur and have been described by DETHLOFF et al. (2006). Figure 9 presents the low-passed filtered Eliassen-Palm flux divergence differences at 850 and 500 hPa for the sensitivity experiment with the ECHO-G model "New albedo minus Control". Along the east Pacific coast a large-scale planetary wave train is clearly visible on both pressure levels as a result of the feedbacks between the westerly wind jets and planetary waves. Changes occur also in the storm tracks over northern America and northern Europe owing to the improved Arctic albedo parameterization.

Changes in the polar energy sink region exert a strong influ-

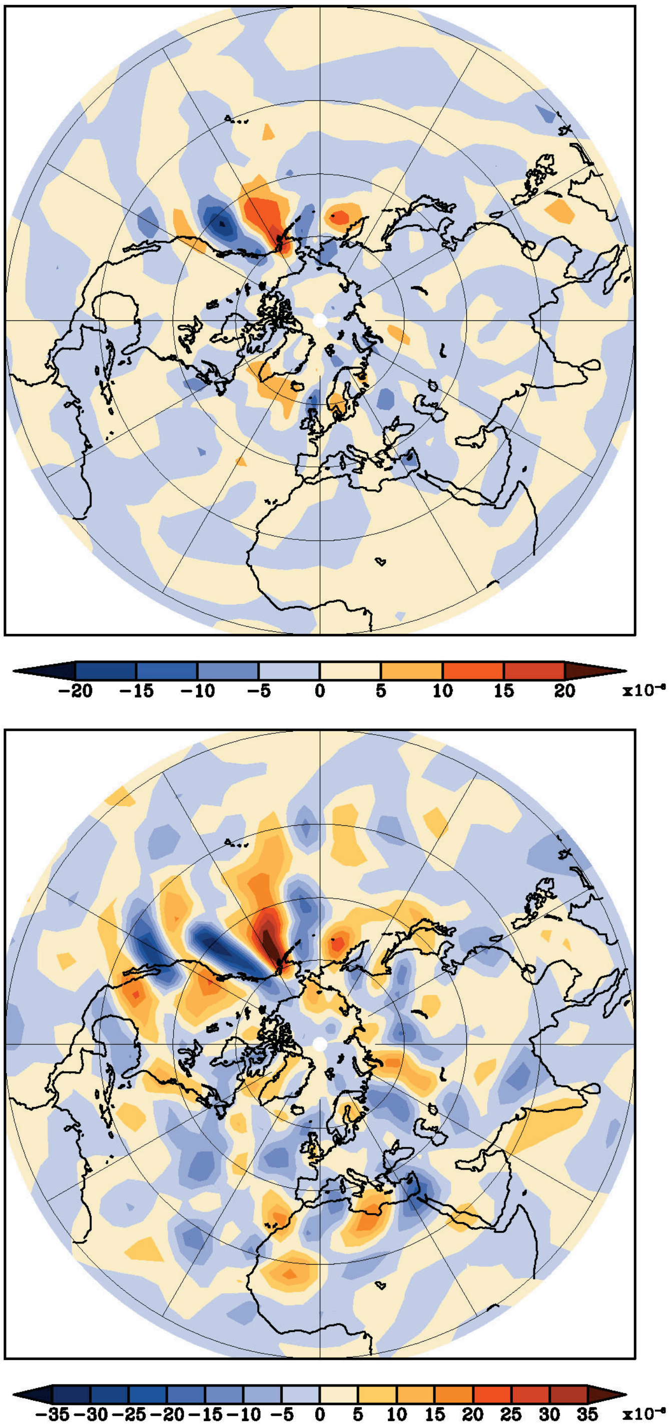

Fig. 9: Differences of the divergence [10^{-6} m s^{-2}] of the localised Eliassen-Palm fluxes at the 850-hPa pressure level (= top) and the 500-hPa pressure level (= bottom) between the "new sea-ice and snow albedo run" and the "control run" of the coupled global climate model ECHO-G. The Eliassen-Palm fluxes were averaged over eight winters (December to February) using low-pass (10-90 days) filtered data.

Abb. 9: Differenz der Divergenz [10^{-6} m s^{-2}] der Eliassen-Palm-Flüsse auf der 850hPa-Druckfläche (= oben) und der 500hPa-Druckfläche (= unten) zwischen dem Lauf mit der neuen Meereis- und Schneealbedo und dem Kontrolllauf des gekoppelten globalen Klimamodells ECHO-G. Die Eliassen-Palm-Flüsse wurden unter Verwendung Tiefpass (10-90 Tage) gefilterter Daten über acht Winter (Dezember bis Februar) gemittelt.

ence on the mid- and high-latitude climate by modulating the strength of the sub-polar westerlies and storm tracks. Disturbances in the wintertime Arctic sea-ice and snow cover induce perturbations in the zonal and meridional planetary wave train from the tropics over the mid-latitudes into the Arctic. This approves, that Arctic processes can feed back on the global climate system via an atmospheric wave bridge between the energy source in the tropics and the energy sink in the polar regions. The atmospheric heat and momentum fluxes on seasonal time scales increase in the middle and high troposphere between 30 and 50 °N as a result of the new sea-ice and snow albedo parameterization of the Arctic. The improved parameterization of Arctic sea-ice and snow albedo in a global climate model exert strong influences on the global geopotential pattern of the middle troposphere and shows similarities with the Arctic Oscillation and North Atlantic Oscillation patterns. This implies an influence on the meridional coupling between the energy sources in the tropics and the energy sink in the Arctic and would have strong implications for CO_2 scenario runs.

500-year long simulations with the state-of-the-art AOGCMs ECHAM4/OPYC and the ECHO-G with the old and the new snow and sea-ice albedo scheme have been carried out and described by BENKEL & KØLTZOW (2006) and STENDEL et al. (2005). The models are driven with most relevant forcings, both natural (solar variability, volcanic aerosol) and anthropogenic (greenhouse gases, sulphate aerosol, land-use changes). Multi-decadal circulation anomalies are seen, e.g., the Maunder Minimum and both models are able to simulate cold and warm 25 year long lasting anomalies as deviations from the 200-year mean 1500-1700.

Global impacts of interactive stratospheric ozone chemistry

The special regional temperature conditions in the cold stratospheric polar vortex over the Arctic contribute mainly to the observed chemical ozone depletion processes. Changes in greenhouse gas concentrations and distributions, be that due to natural variability or anthropogenic influence, exert a strong impact on global climate. Since, in turn, stratospheric ozone formation and destruction are highly temperature dependent, dynamical changes are significantly affecting atmospheric chemistry. For example, a cooling in the stratosphere, connected with global tropospheric warming, would slow down the overall stratospheric gas phase chemistry, but at the same time enhance catalytic ozone destruction in the polar lower stratosphere, where heterogeneous chlorine activation on Polar Stratospheric Clouds (PSCs) would be intensified. To account for such complex, nonlinear dependencies a coupled atmosphere–ocean–sea-ice model including interactive chemistry is needed.

Therefore, a new Atmosphere–Ocean General Circulation Model (AOGCM) with simplified stratospheric chemistry, ECHO-GiSP, has been developed by BRAND et al. (2007, 2008). A main focus of ECHO-GiSP is the integration of the coupled atmosphere–ocean system with a tropo- and stratospheric chemistry. This aims to investigate interactions between the atmospheric model dynamics and tracer distributions and concentrations, e.g., leading to a better understanding of basic feedback effects between chemistry and dynamics.

ECHO-GiSP is based on an ECHO-G middle atmosphere version (39 levels up to 80 km) and the MECCA chemistry module. A central feature of the new model is the so-called Integrated Stratospheric Chemistry (ISC), which allows a free choice of chemical tracers and equations for each model simulation, and automatically prepares the related model source code. In order to be able to keep the chemistry scheme on a more simplified level, but additionally depending on computational resources, it is also possible to restrict the simulation of the tracer concentrations only to the upper tropospheric and stratospheric model levels.

The chemistry configuration for the simulations is a setup with 39 chemical species for which 116 chemical reactions are defined (81 gas phase reactions, 25 photolysis reactions and 10 heterogeneous reactions on Polar Stratospheric Cloud (PSC). The species include the main members of the Ox, NOx, ClO_x, HO_x and BrO_x chemical families, as well as other atmospheric gases like CO, CO_2, CH_4, N_2, and H_2. The "reference run" (REF) treated the chemistry scheme as a passive part of the model, i.e. itself depending on the dynamical model variables, but without any feedback to them. In contrary, the "coupled run" (COUP) simulated the ozone concentrations interactively within the radiation scheme instead using the prescribed parameterizations and prescribed ozone profiles considered in the reference run.

Model runs focusing on decadal variability can be performed using this restricted chemistry domain, since in terms of decadal variability especially the feedback between stratospheric chemistry and dynamics has to be examined. For such runs the tropospheric sources and sinks have to be prescribed, including chemical boundary conditions at the respective levels as well as the initial conditions on all 39 levels. Therefore, for each chemical species and each grid point a set of parameters was fitted in order to describe the mean annual and mean semi-annual variations for that species by an idealized cyclic function. By this means, the chemical boundary conditions can be provided time-dependent, leading to a more realistic transport of tracer mass into the higher levels of the stratosphere where the chemistry is calculated explicitly.

With the ECHO-GiSP model, two 150-year climate simulations were performed in order to enable us to focus on coupling mechanisms between stratospheric ozone chemistry and dynamical processes on interannual to decadal scales. The results from these simulations indicate significant circulation changes in the tropo- and stratosphere due to interactive stratospheric ozone feedbacks, which were enabled in COUP, but neglected in REF. This means, that the reference run only included the dependency of chemistry on the model dynamics, while the coupled run also included the feedback effect from the tracer concentrations back to the model dynamics. This feedback takes place via radiation processes.

The validation shows, that the tropospheric and stratospheric jets occur with the right position and strength in the model, which also forms a well developed polar vortex. Further, the tropospheric circulation cells and the interhemispheric Brewer-Dobson meridional mean circulation in stratosphere and mesosphere appear realistically. There are various differences between the two runs, e.g., there is a lower maximum value of the ozone concentrations in the interactive simulation as well as stronger tropospheric and weaker strato-mesospheric jetstream(s) (Fig. 10a).

One particular result is that the decadal variability within the runs is influenced by the AO mode. Moreover, Brand et al. (2008) showed that in the interactive simulation, i.e. with enabled interactive stratospheric chemistry, the atmospheric circulation generally tends to the negative AO phase. Especially, there is a clear sensitivity of the tropospheric circulation dynamics to the stratospheric chemistry in the Arctic. This also includes an enhanced mid-latitudinal planetary and synoptic scale wave activity. The strengthening of the synoptic scale waves leads to stronger storm tracks over the Atlantic Ocean, while the planetary scale waves show larger changes outside. Another region, influenced by interactive stratospheric chemistry effects, is the tropical troposphere where a significant cooling appears in the positive AO phase compared to the negative phase. This tropical tropospheric cooling is related to a concurrent warming in the tropical lower stratosphere due to changes in lower stratospheric ozone concentrations. Generally, compared with the reference simulation, the tropospheric variability within the interactive simulation

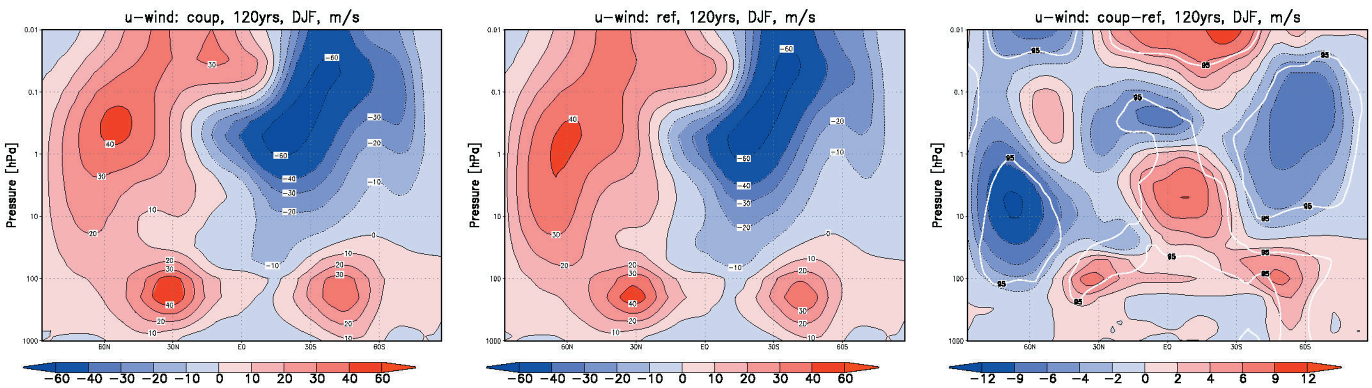

Fig. 10a: Latitude-height cross-section of zonal mean zonal wind [m s^-1] in winter (December to February) averaged over model years 31 to 150 from simulations of the coupled model ECHO-GiSP. The model simulations were carried out with interactive chemistry (= left) and with prescribed chemistry (= middle), respectively. The difference between the two simulations is shown in the right panel.

Abb. 10a: Breiten-Höhen-Schnitt des zonal gemittelten Zonalwindes [m s^-1] im Winter (Dezember bis Februar) der Modelljahre 31 to 150 aus Simulationen des gekoppelten Modells ECHO-GiSP. Die Modellsimulationen wurden mit interaktiver Chemie (= links) beziehungsweise mit vorgeschriebener Chemie (= Mitte) durchgeführt. Die Differenz zwischen beiden Simulationen ist im rechten Teilbild dargestellt.

appears to be enhanced, while the strato-mesospheric variability weakens.

Changes in the atmospheric variability mode of the AO also imply changes in the planetary and synoptic scale wave activity. This is confirmed by Figure 10b, where results of a discrete Fourier transform (DFT) for the northern hemisphere low-pass (10-90 days) and band-pass (2-6 days) filtered geopotential data at 500 hPa are displayed. The mean power (logarithm of squared wave amplitude) for the wave-numbers 1-3 (with low-pass filtered data) generally shows an increase in “COUP” relative to “REF”, but with local maxima around 65 °N and 45 °N and a minimum near 55 °N. In contrast, the synoptic scale wave-numbers 4-10 (with band-pass filtered data) have only one broad maximum (increase of wave activity) between 50-60 °N. Hence, locally the strengthening of the mid-latitudinal storm tracks is anti-correlated to the planetary wave activity. Globally, however, “COUP” appears with enhanced tropospheric wave activity compared to “REF”.

The stability of the stratospheric polar vortex is reduced in the interactive runs. In mid- and high latitudes there is a dependency of tropospheric circulation and surface climate on the stratospheric variability. In agreement with the conclusions by Stenchikov et al. (2002), this implies a positive feedback loop between the stratospheric polar vortex, the tropospheric mid-latitude zonal mean flow, the associated planetary wave activity and its effect back on the stratospheric polar vortex as a possible coupling mechanism. The tropospheric shift to a negative AO phase in interactive model simulations could therefore be due to the stratospheric stabilizing effect of the coupling between chemistry and dynamics, which leads to weaker meridional temperature gradients and thus to a weaker polar vortex.

Atmospheric two-way feedbacks

Modelling atmospheric flows for climate simulations as well as for weather prediction is a complex problem due to the nonlinear structure of the dynamical and physical phenomena on widely varying spatial and temporal scales and their multi-scale interaction processes. For the large-scale flow, e.g., the interaction between meso-scale flow instabilities and the planetary Rossby waves plays a crucial role for climate variability on time-scales from seasons to decades. Improved discrete representations of these nonlinear phenomena contribute to the understanding of natural climate variability and thus to the achievement of reliable assessments of future climate development and the impact of anthropogenic influence. Within this section, this complex problem is discussed within the scope of a global atmospheric model with an unstructured adaptive grid.

The regional climate model simulations, described within this article, consider only a simple one-way feedback and do not allow for two-way dynamical feedbacks, especially from the regional to the global scale. To overcome this deficit and to allow multi-scale interaction processes like those between the planetary and barotropic waves with meso-scale circulation structures, a parallel adaptive model of the atmosphere PLASMA has been developed and described by Läuter et al. (2007). For the discretization of the underlying spherical shallow water equations, the adaptive Lagrange-Galerkin

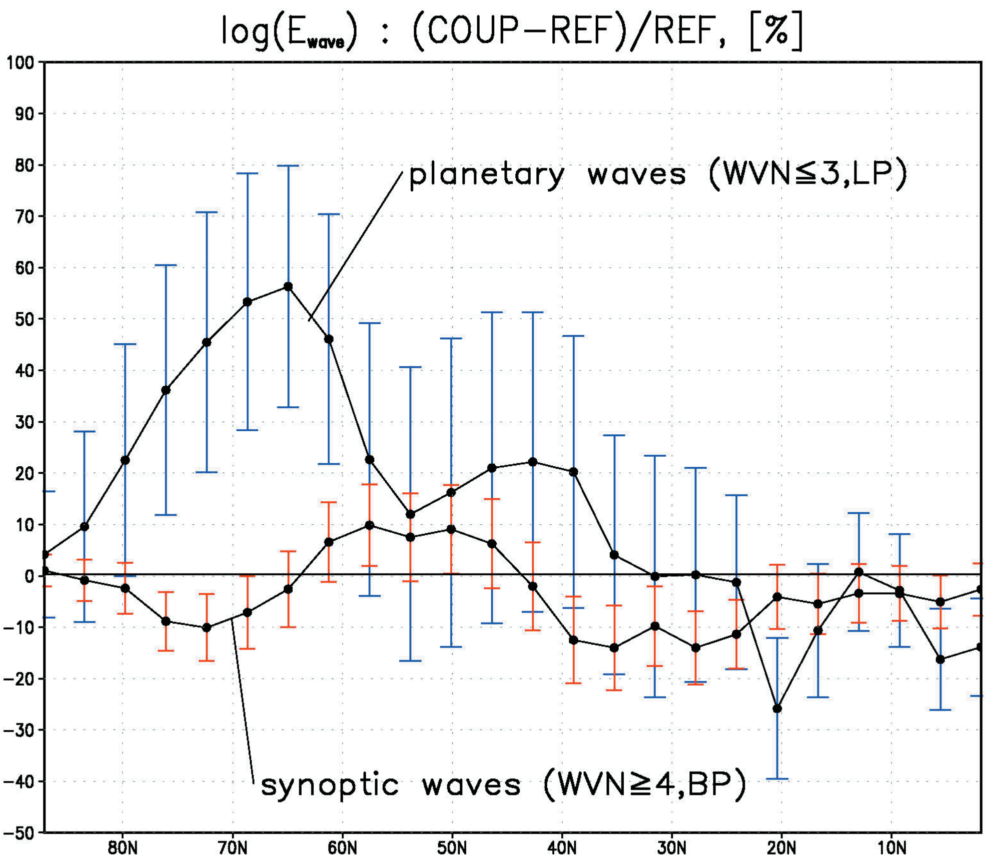

Fig. 10b: Relative differences of the logarithm of the wave energy [%] between the model simulation with interactive chemistry and the reference simulation in relation to the reference simulation. The wave energy was calculated using Discrete Fourier Transform (DFT) of the Northern Hemisphere 500-hPa geopotential height fields in the wintertime (December to February) of the model years 31 to 150. The relative differences are shown for low-pass (10-90 days) filtered wave numbers (WVN) 1-3 and band-pass (2-6 days) filtered WVN 4-10. The error bars show the 1-standard-deviation uncertainties based on yearly data.

Abb. 10b: Relative Differenzen des Logarithmus der Wellenenergie [%] zwischen der Modellsimulation mit interaktiver Chemie und der Referenzsimulation in Bezug auf die Referenzsimulation. Die Wellenenergie wurde durch Diskrete Fourier-Transformation (DFT) der nordhemisphärischen 500 hPa-Geopotenzial-Felder in den Wintermonaten (Dezember bis Februar) der Modelljahre 31 bis 150 berechnet. Die relativen Differenzen sind für Tiefpass (10-90 Tage) gefilterte Wellenzahlen (WVN) 1-3 und Bandpass (2-6 Tage) gefilterte WVN 4-10 dargestellt. Die Fehlerbalken zeigen die Unsicherheiten bezogen auf die Standardabweichung jährlicher Daten.

method, a combination of the finite element method and the semi-Lagrangian method, has been employed. The unstructured triangular grid is generated with the grid generator "amatos", and the large linear systems have been solved.

Convergence studies show the first order approximation for steady-state analytical solutions as well as for unsteady analytical solutions (see WILLIAMSON et al. 1992, LÄUTER et al. 2005). PLASMA shows satisfactory results in the quasi-standard experiments with the Rossby-Haurwitz and the planetary Rossby wave generation within a zonal flow over an isolated mountain. Both uniform grid experiments and adaptive grid experiments can be performed with PLASMA. In the adaptive case the computational grid is adapted at each time step according to a physical error estimator. The comparison of uniform and adaptive grid experiments documents that the adaptive model leads to a significant reduction of the number of grid points while the numerical error increases only slightly. For the realization of adaptive atmospheric simulations from seasonal up to annual time scales, the model needs to be further improved. Longer model integrations require a discrete conservation of the physical variables mass, energy and potential enstrophy. Furthermore, the physical error estimator could be further improved, especially inside turbulent flow structures. Finally, the application of the adaptive grid in PLASMA can be assigned to a baroclinic multi-layer model.

To improve the conservation properties on the unstructured adaptive grid, which are important especially for long-term climate model simulations, a high order Runge-Kutta discontinuous Galerkin method for the shallow water equations has been developed by LÄUTER et al. (2008). The model has been validated in terms of standard tests for shallow water models and a further demanding test by GALEWSKI et al. (2004), describing a barotropic instability caused by a very small initial perturbation. Adaptive grid experiments can be performed by choosing any conformal triangulation of the sphere.

Figure 11a shows a quasi-uniform grid with a resolution of 133 km and an adaptive grid with a higher resolution of 67 km in the polar region. For the model experiments in this section, the earth orography is zero, except for an idealized orography of Greenland. Using the adaptive grid, this orographic forcing is better resolved compared to the uniform grid. In the geostrophically balanced field of a westerly wind with a meridional distribution of a solid body rotation (the maximum wind speed is 20 m s^{-1}), Greenland's orography forces a Rossby

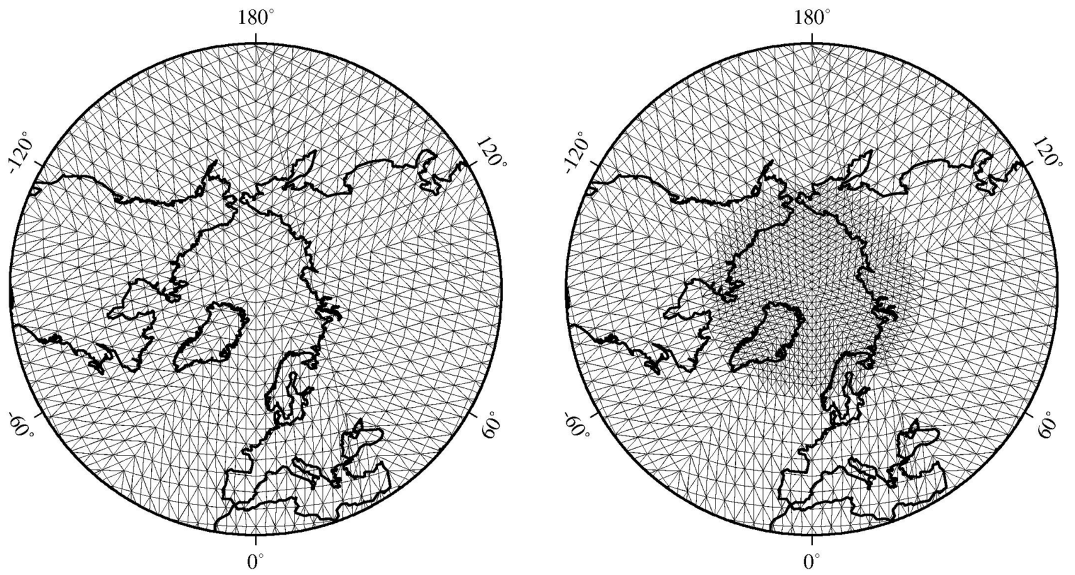

Fig. 11a: Unstructured adaptive model grids; (left) = quasi-uniform grid with resolution of 133 km; (right) = adaptive grid with enhanced resolution of 67 km in the polar region.

Abb. 11a: Unstrukturierte adaptive Modellgitter, (links) = quasi-homogenes Gitter mit Auflösung von 133 km, (rechts) = adaptives Gitter mit erhöhter Auflösung von 67 km in der Polarregion.

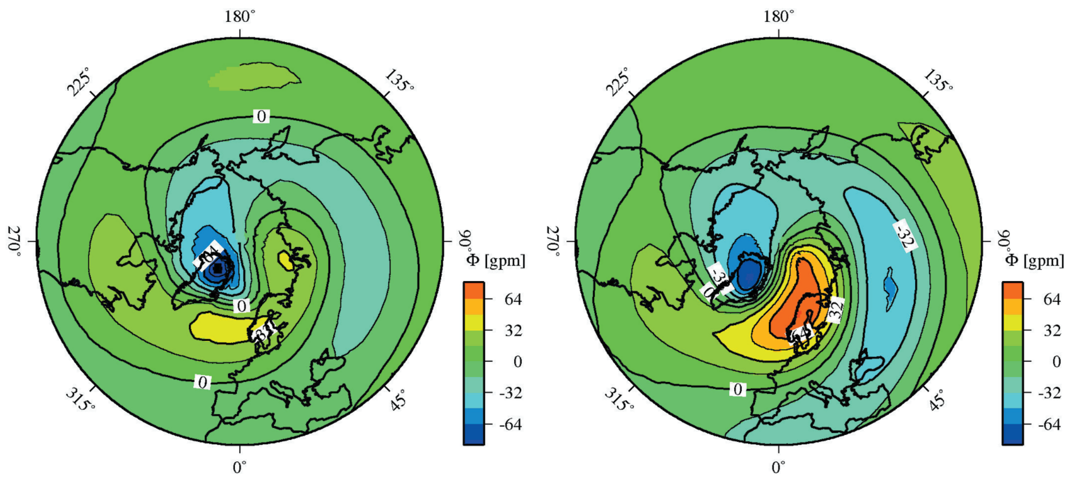

Fig. 11b: Deviations in simulated geopotential heights [gpm] from an initially geostrophically balanced field after 30 days due to an orographic perturbation; (left) = quasi-uniform grid experiment; (right) = adaptive grid experiment.

Abb. 11b: Abweichungen in den simulierten geopotenziellen Höhen [gpm] von einem anfänglich geostrophisch ausbalancierten Feld nach 30 Tagen infolge einer orografischen Störung; (links) = Experiment mit quasihomogenem Gitter; (rechts) = Experiment mit adaptivem Gitter.

wave structure. Figure 11b shows the geopotential height perturbations after 30 days. Qualitatively, the uniform and the adaptive grid experiment agree on the large-scale planetary wave structure caused by the mountain perturbation. Anyway, the higher polar grid resolution leads to stronger height gradients, which causes perturbation amplification even beyond the boundary of the high resolution area. This effect makes clear that an improved regional grid resolution will affect the planetary wave structure if the multi-scale interaction from the regional to the global scale is considered in the model.

CONCLUSIONS AND OUTLOOK

GCMs constitute the primary tool for capturing the behaviour of the Earth's climate system, but atmospheric and coupled RCMs with high spatial and temporal resolution are more accurate in polar regions than GCMs with relatively low resolution. RCMs can provide added value at small scales to the climate statistics when driven by GCM outputs at the lateral and lower boundaries, assuming that GCMs are accurate on large scales. In the data sparse polar regions, RCMs are often used as intelligent data interpolator.

As shown by STROEVE et al. (2007), IPCC AR4 models incorporate many improvements compared to their predecessors, but shortcomings still remain. While some studies suggest anthropogenic forcing may favour a positive Northern Annular Mode (NAM), there is evidence that climate models underestimate NAM-like variability, as discussed by STENCHIKOV et al. (2006). MASLANIK et al. (2007) analysed three types of atmospheric circulation patterns, which appear most significant in terms of Arctic basin winds and ice transport. The "light ice" phases of these patterns include decreased SLP in the North Atlantic (an "NAO-like" pattern resembling the positive phase of the NAO), a low-pressure cell within the Arctic basin (a "central Arctic" pattern), and a dipole pattern of high pressure over the Canadian Arctic paired with low pressure over the Siberian Arctic. Winds and ice transport patterns that favour reduced ice cover in the western and central Arctic have in fact continued to be present since the late 1980s, but the AO index is not a reliable indicator of these patterns. Hence, regional atmospheric circulation remains a significant factor of recent reductions in ice cover. The observed strong Arctic warming over the last few decades can be attributed to increased greenhouse gas concentrations and the strong natural variability in the coupled ice–ocean–atmosphere system.

RCMs can be used as an intelligent data interpolator in the data sparse polar regions and can help to attribute the origin of ongoing changes in the Arctic climate system. RCMs can deliver valuable input for improving the performance of global climate models, especially in the Arctic. The influences of atmosphere–ocean–sea-ice and atmosphere–land–soil interactions in coupled RCM simulations have been investigated. These deliver valuable information by improving the physical realism of the considered physical feedback processes. Sensitivity studies concerning the sea-ice–albedo feedback, the stable stratified planetary boundary layer, aerosols, clouds and radiation, sea-ice–atmosphere–ocean coupling and permafrost-atmosphere interactions have been carried out.

Although much of the resolved-scale regional atmospheric dynamics is quite well captured by the RCMs there are biases in the near-surface wind speed that are consistent with biases in surface momentum fluxes. There are also errors in the surface heat fluxes connected with biases in the radiation flux components. This indicates the need for improved planetary boundary layer parameterizations meeting the specific polar conditions. As pointed out by WYSER et al. (2007) for the ARCMIP, the inter-model spread of simulated cloud cover is very large, with no model appearing systematically superior. Analysis of the co-variability of terms controlling the surface radiation budget reveal some of the key processes requiring improved treatment in Arctic RCMs, especially the parameterizations of cloud cover and cloud microphysical optical parameters, surface albedo and solar transmissivity to better match the observations, thereby more faithfully representing the key physics controlling the Arctic surface radiation.

There are very good reasons to assume that some of the errors in the boundary layer and at the surface have their roots elsewhere in unrealistic description of regional model feedbacks. Taking into account the discussed uncertainties in modelling the Arctic climate by RCMs it is unlikely that formulations in current GCMs are in general much better than in the state-of-the-art regional climate models evaluated here. Therefore, it would appear prudent to consider scenario results of future Arctic climate in particular ice-melt scenarios, with considerable caution.

We identified a set of improvements needed for Arctic models. Some of these recommendations are common for all models and are "trivial" but need serious attention, namely: increasing of model resolution, better initial and boundary conditions, and improved forcing. The atmospheric models can be improved by better description and parameterization of cloud properties, surface turbulent fluxes and especially convective plumes associated with polynyas and leads. Climate effects representing tropospheric aerosols and clouds, stratospheric ozone have to be studied in greater details and improved. Significant improvements are needed in the description of precipitation processes and humidity fluxes. Surface radiative fluxes, spatial and temporal variability of snow and ice albedo, thorough and detail studies of inversions and stable boundary layer are also important for model improvements.

Coupled atmosphere–sea-ice–ocean and coupled atmosphere–soil models have been improved. It was shown that the treatment of snow layer on sea ice is a very important factor for ice-melt during summer. Processes of vertical and lateral mixing, parameterization of eddies, plumes, freshwater transformations and fluxes have to be improved and validated. With the increase of model horizontal resolution the sea-ice and snow dynamics and thermodynamics have to be improved toward better description of small-scale processes and deformations, and introduction of forcing at inertial and tidal frequencies. Land-fast ice development and decay has to be taken into account as well. Reduction of uncertainties in terrestrial land and soil model results can be reached via improvements of information about evapotranspiration, soil characteristics, precipitation and moisture fluxes, better permafrost models and permafrost characteristics and processes in wetlands and peatlands.

The global impact of improved Arctic sea-ice albedo parameterization and the global influences of an interactive stratospheric chemistry in the Arctic polar vortex have been investigated. Disturbances in the wintertime Arctic sea-ice and snow cover induce perturbations in the zonal and meridional planetary wave train from the tropics over the mid-latitudes into the Arctic. The atmospheric heat and momentum fluxes on seasonal time scales increase in the middle and high troposphere between 30 and 50 °N as a result of the new sea-ice and snow albedo parameterization of the Arctic. The improved parameterization of Arctic sea-ice and snow albedo in a global climate model exert strong influences on the global geopotential pattern of the middle troposphere and shows similarities with the Arctic Oscillation and North Atlantic Oscillation patterns. This implies an influence on the meridional coupling between the energy sources in the tropics and the energy sink in the Arctic and would have strong implications for CO_2 scenario runs. GCM simulations with interactive stratospheric ozone chemistry in the Arctic show significant differences to the reference run with prescribed chemistry with respect to dynamic features as the appearance and variability of the tropospheric and stratospheric jets or the connected wave activity. In the troposphere, the coupled run, including interactive chemistry feedbacks, tends to the negative phase of the AO, including stronger subtropical jets and a stronger meridional mean circulation. This is connected with warmer stratospheric conditions and a weaker, more disturbed polar stratospheric vortex. The coupled run generally occurs with enhanced tropospheric variability, whereas the stratospheric and mesospheric variability shows the opposite behaviour.

The regional climate model simulations consider only dynamical one-way feedbacks and do not allow for two-way dynamical feedbacks. To overcome this deficit and to allow multi-scale interaction processes a parallel adaptive global model of the atmosphere has been developed.

The application of a hierarchical approach discussed in this paper, including uncoupled models of the Arctic and Antarctic atmosphere and coupled Arctic regional climate system models together with global coupled climate models, can help to attribute the current changes and to understand the consequences of Arctic warming. This concerns the shrinking of summer sea ice, changes in atmospheric circulation patterns, cloud cover and water vapour changes, melting of permafrost, changes in ice transport in response to atmospheric winds and ocean currents, stratospheric ozone reduction, the ocean–shelf-ice interaction including deep water formation, stability of shelf-ice, sea level, and changes in ocean heat transports.

Qualitative and quantitative consequences of these changes for ocean, atmosphere, and ecosystems are obvious, and impacts on global climate are unavoidable. Warming will lead to melting of permafrost and thus to further release of methane and to changes of atmosphere and ocean circulation that may affect the uptake of CO_2 by the Ocean. The understanding of the polar climate system is still incomplete due to its complex atmosphere–land–cryosphere–ocean–ecosystem interactions involving a variety of distinctive feedbacks. In particular clouds, aerosols and ozone, planetary boundary layer processes, sea ice, and marine ecosystems are not well represented in climate models (IPCC 2007). On annual and decadal timescales, the various earth system components interact mainly via the atmosphere, the upper ocean dynamics (circulation, waves, mixing), greenhouse gases (H_2O, CO_2, CH_4) and energy and moisture fluxes.

With respect to the Arctic, further investigations in the following directions are needed:
(i) Development and improvement of regional models of the coupled Arctic and Antarctic climate systems, including the climate subsystems atmosphere, ocean, sea ice, land and permafrost, and glaciers and their interactions with terrestrial and marine ecosystems.
(ii) Improvement of the model performance in close collaboration of experimental and modelling activities during the IPY and carrying out atmospheric and oceanic measurements in different key regions of the Arctic.
(iii) Process and feedback understanding of Arctic climate variations and observed variability patterns for improved description of atmospheric processes on seasonal to decadal time scales in global climate models.
(iv) Determination of the impact of polar regions and regional polar feedbacks as key drivers for global climate changes and reduction of the uncertainties of future climate change scenarios.

ACKNOWLEDGMENTS

This paper is based on an invited talk at the DACH Meteorologentagung on 11th September 2007 in the session “Meteorologie der hohen Breiten”. The authors would like to thank an anonymous reviewer for helpful advices, which improved the manuscript, and Prof. D. Fütterer for his insightful editorial work.

List of abbreviations

AARI	Arctic and Antarctic Research Institute, St. Petersburg
AO	Arctic Oscillation
AOE-2001	Arctic Ocean Experiment 2001
AOGCM	Atmosphere-Ocean General Circulation Model
AON	Arctic Observational Network
ARCMIP	Arctic Regional Climate Model Intercomparison Project
ARCSyM	Arctic Region Climate System Model
AVHRR	Advanced Very High Resolution Radiometer
AWI	Alfred Wegener Institute
COAMPS	Coupled Ocean-Atmosphere Mesoscale Prediction System
COUP	ECHO-GiSP coupled simulation with interactive chemistry
CRCM	Canadian Regional Climate Model
DFT	Discrete Fourier Transform
ECHAM	European Centre Hamburg Model (global atmosphere model)
ECHAM3/4	ECHAM, 3rd generation/4th generation
ECHAM3_MO	HIRHAM simulation using ECHAM3 physics with Monin-Obukhov similarity theory for the PBL
ECHAM3_RO	HIRHAM simulation using ECHAM3 physics with Rossby-number similarity theory for the PBL
ECHO-G	ECHAM4 + HOPE-G (AOGCM)
ECHO-GiSP	ECHO-G with Integrated Stratospheric Chemistry
ECMWF	European Centre for Medium-Range Weather Forecasts
EOF	Empirical Orthogonal Function
ERA/ERA-40	ECMWF Reanalysis (40 years)
GCM	General Circulation Model
HIRHAM	High-Resolution Limited Area Model + ECHAM physics
HIR-LSM	HIRHAM coupled with LSM
HOPE-G	Hamburg Ocean Primitive Equation model, Global version
IPCC	Intergovernmental Panel on Climate Change
IPCC AR4	IPCC Fourth Assessment Report (2007)
IPY	International Polar Year (2007–2009)
ISC	Integrated Stratospheric Chemistry
JRA-25	Japanese 25-year Reanalysis
LBC	Lateral Boundary Condition

LSM	Land Surface Model
MECCA	Module Efficiently Calculating the Chemistry of the Atmosphere
met.no	Norwegian Meteorological Institute
MIP	Model Intercomparison Project
MOM-2	Modular Ocean Model, 2nd generation
MPI	Max Planck Institute
MSLP	Mean Sea-Level Pressure
NAM	Northern Annular Mode
NAO	North Atlantic Oscillation
NAOSIM	North Atlantic/Arctic Ocean Sea Ice Model
NASA	National Aeronautics and Space Administration
NCAR	National Center for Atmospheric Research
NCEP	National Centers for Environmental Predictions
NH	Northern Hemisphere
NOAA	National Oceanic and Atmospheric Administration
NP	North Pacific index
OPYC	Ocean isoPYCnal model
PBL	Planetary Boundary Layer
PDO	Pacific Decadal Oscillation
PLASMA	Parallel LArge-scale Self-adaptive Model of the Atmosphere
PolarMM5	Polar Mesoscale Model, 5^{th} generation
PSC	Polar Stratospheric Cloud
PV	Polar Vortex
RCA	Rossby Centre regional Atmosphere model
RCM	Regional Climate Model
REF	ECHO-GiSP reference simulation with passive chemistry
RegCM	Regional Climate Model of met.no
REMO	REgional climate MOdel of MPI Hamburg
SAM	Southern Annular Mode
SAT	Surface Air Temperature
SCM	Single-Column Model
SHEBA	Surface Heat Budget of the Arctic Ocean
SMHI	Swedish Meteorological and Hydrological Institute
SSM/I	Special Sensor Microwave/Imager
SST	Sea Surface Temperature
TKE	Turbulent Kinetic Energy

References

Arfeuille, G., Mysak, L.A. & Tremblay, L.-B. (2000): Simulation of the interannual variability of the wind-driven Arctic sea-ice cover during 1958-1998.- Clim. Dyn. 16: 107-121.

Barry, R., Zhang, T. & Gilichinsky, D. (2001): Russian historical soil temperature data, digital media.- Natl. Snow and Ice Data Cent., Boulder, Colorado.

Benkel, A. & Køltzow, M. (2006): A new sea-ice albedo parameterization in ECHO-G and its global consequences.- In: A. RINKE & K. DETHLOFF (eds), Global Implications of Arctic Climate Processes and Feedbacks. Rep. Polar Mar. Res. 520: 9-12.

Betts, R.A. (2000): Offset of the potential carbon sink from boreal forestation by decreases in surface albedo.- Nature 408: 187-190.

Bonan, G.B. (1996): A land surface model (LSM version 1.0) for ecological, hydrological and atmospheric studies: Technical description and user's guide.- Tech. Rep. NCAR/TN-417+STR.- Natl. Cent. Atmos. Res., Boulder, Colorado, 150 pp.

Bonan, G.B. (1998): Sensitivity of a GCM simulation to inclusion of inland water surfaces.- J. Clim. 8: 2691-2704.

Box, J.E. & Rinke A. (2003): Representation of Greenland ice sheet surface climate in the HIRHAM regional climate model.- J. Clim. 16: 1302-1319.

Brand, S., Dethloff, K. & Handorf, D. (2007): Atmospheric variability in a coupled atmosphere–ocean–sea ice model with interactive stratospheric ozone chemistry.- The Open Atmos. Sci. J. 1: 6-19, doi:10.2174/1874282300701010006.

Brand, S., Dethloff, K. & Handorf, D. (2008): Tropospheric circulation sensitivity to an interactive stratospheric ozone.- Geophys. Res. Lett. 35: L05809, doi:10.1029/2007GL032312.

Bromwich, D.H., Cassano, J.J., Klein, T., Heinemann, G., Hines, K.M., Steffen, K. & Box, J.E. (2001): Mesoscale modelling of katabatic winds over Greenland with the Polar MM5.- Mon. Wea. Rev. 129: 2290-2309.

Bromwich, D.H., Guo, Z., Bai, L. & Chen, Q.-S. (2004): Modelled Antarctic Precipitation. Part I: Spatial and temporal variability.- J. Clim. 17: 427-447.

Bromwich, D.H., Fogt, R.L., Hodges, K.I. & Walsh, J.E. (2007): A tropospheric assessment of the ERA-40, NCEP, and JRA-25 global reanalyses in the polar regions.- J. Geophys. Res.: 112, doi:10.1029/2006JD007859.

Cassano, J.J., Box, J.E., Bromwich, D.H., Li, L. & Steffen, K. (2001): Evaluation of Polar MM5 simulations of Greenland's atmospheric circulation.- J. Geophys. Res. 106: 33867-33889.

Casty, C., Handorf, D., Raible, C.C., Gonzalez-Rouco, J.F., Weisheimer, A., Xoplaki, E., Luterbacher, J., Dethloff, K. & Wanner, H. (2005): Recurrent climate winter regimes in reconstructed and modelled 500 hPa geopotential height fields over the North Atlantic/European sector 1659-1990.- Climate Dyn. 24: 809–822, doi:10.1007/s00382-004-0496-8.

Caya D. & Biner, S. (2004): Internal variability of RCM simulations over an annual cycle.- Clim. Dyn. 22: 33-46.

Cavalieri D., Gloerson P., & Zwally J. (1990, updated 2004): DMSP SSM/I monthly polar gridded sea-ice concentrations, 1988 to 2003.- In: J. MASLANIK & J. STROEVE (eds), Natl. Snow and Ice Data Cent., Boulder, Colorado, Digital media.

Christensen, J.H. et al. (2007): Regional climate projections, Climate Change, 2007: The physical science basis. Contribution of Working group I to the Fourth Assessment Report of the Intergovernmental Panel on Climate Change, University Press, Cambridge, Chapter 11: 847-940.

Comiso J. (2002): Bootstrap sea-ice concentrations for NIMBUS-7 SMMR and DMSP SSM/I.- Natl. Snow and Ice Data Cent., Boulder, Colorado, Digital media. <http://www.nsidc.org/data/nsidc-0079.html>

Committee on designing an AON (2006): Toward an integrated Arctic Observing Network.- Nat. Academic Press, Washington, 129 pp.

Corti, S., Molteni, F. & Palmer, T.N. (1999): Signature of recent climate change in frequencies of natural atmospheric circulation regimes, Nature 398: 799-802.

Curry, J.A. & Lynch, A.H. (2002): Comparing arctic regional climate models.- EOS Trans. 83: 87.

Curry, J.A., Schramm, J. & Ebert, E.E. (1995): On the sea-ice albedo climate feedback mechanism.- J. Clim. 8: 240-247.

Davis, C.H., Li, Y., McConnell, J.R., Frey, M.M. & Hanna, E. (2005): Snowfall-driven growth in East Antarctic Ice Sheet mitigates recent sea-level rise.- Science 308: 1898-1901.

Dethloff, K., Abegg, C., Rinke, A., Hebestadt, I. & Romanov, V. (2001): Sensitivity of Arctic climate simulations to different boundary layer parameterizations in a regional climate model.- Tellus 53 A: 1-26.

Dethloff, K., Dorn, W., Rinke, A., Fraedrich, K., Junge, M., Roeckner, E., Gayler, V., Cubasch, U. & Christensen, J.H. (2004): The impact of Greenland's deglaciation on the Arctic circulation.- Geophys. Res. Lett. 31: L19201, doi:10.1029/2004GL020714.

Dethloff, K. et al. (2006): A dynamical link between the Arctic and the global climate system.- Geophys. Res. Lett. 33: L03703, doi:10.1029/2005GL02524.

Dethloff, K., Rinke, A., Lehmann, R., Christensen, J.H., Botzet, M. & Machenhauer, B. (1996): Regional climate model of the Arctic atmosphere.- J. Geophys. Res. 101: 23401-23422.

Dorn, W., Dethloff, K., Rinke, A. & Roeckner, E. (2003): Competition of NAO regime changes and increasing greenhouse gases and aerosols with respect to Arctic climate projections.- Clim. Dyn. 21: 447-458, doi:10.1007/s00382-003-0344-2.

Dorn, W., Dethloff, K., Rinke, A., Frickenhaus, S., Gerdes, R., Karcher, M. & Kauker, F. (2007): Sensitivities and uncertainties in a coupled regional atmosphere–ocean–ice model with respect to the simulation of Arctic sea ice.- J. Geophys. Res. 112: D10118, doi:10.1029/2006JD007814.

Dorn, W., Dethloff, K., Rinke, A. & Kurgansky, M. (2008): The recent decline of the Arctic summer sea-ice cover in the context of internal climate variability.- The Open Atmos. Sci. J. 2: 91-100, doi:10.2174/1874282300802010091.

Flato, G.M. and Participating CMIP Modelling Groups (2004): Sea-ice and its response to CO_2 forcing as simulated by global climate models.- Clim. Dyn. 23: 229-241.

Galewsky, J., Scott, R.K. & Polvani, L.M. (2004): An initial-value problem for testing numerical models of the global shallow water equations.- Tellus A 56: 429-440.

Glushak, K. (2008): Atmospheric circulation and the surface mass balance in a regional climate model of Antarctica.- Diss. Thesis Univ. Potsdam, 158 pp.

Giorgi, F. (1991): Sensitivity of simulated summertime precipitation over western United States to different physics parameterization.- Mon. Wea. Rev. 119: 2870-2888.

Girard, E. & Blanchet, J.-P. (2001): Microphysical parameterization of Arctic diamond dust, ice fog and thin stratus for climate models.- J. Atmos. Sci. 58: 1181-1198.

Holland, M.M. & Bitz, C.M. (2003): Polar amplification of climate change in coupled models.- Clim. Dyn. 21: 221-232, doi:10.1007/s00382-003-0332-6.

Hurrell, J.W. (1996): Influence of variations in extratropical wintertime teleconnections on northern hemisphere temperatures.- Geophys. Res. Lett. 23: 665-668.

Johannessen, O.M., Bengtsson, L., Miles, M.W., Kuzmina, S.I., Semenov, V. Alekseev, G.V., Nagurny, A.P., Zakharov, V.F., Bobylev, L.P., Pettersson, L.H., Hasselmann, K. & Cattle, H.P. (2004): Arctic climate change: observed and modelled temperature and sea-ice variability.- Tellus A, 56: 328-341.

Key J. (2001): The cloud and surface parameter retrieval (CASPR) system for polar AVHRR data user's guide.- Space Science and Engineering Center, Univ. Wisconsin, Madison, 62 pp.
Køltzow M., Eastwood S. & Haugen J. E. (2003): Parameterization of snow and sea ice albedo in climate models.- Res. Rep. 149, Norwegian Meteorol. Inst., Oslo, Norway, 37 pp.
Läuter, M., Giraldo, F.X., Handorf, D. & Dethloff, K. (2008): A discontinuous Galerkin method for the shallow water equations in spherical triangular coordinates.- J. Comp. Phys. 227: 10226-10242, doi:10.1016/j.jcp.2008.08.019.
Läuter, M., Handorf, D. & Dethloff, K. (2005): Unsteady analytical solutions of the spherical shallow water equations.- J. Comp. Phys. 210: 535-553.
Läuter, M., Handorf, D., Rakowsky, N., Behrens, J., Frickenhaus, S., Best, M., Dethloff, K. & Hiller, W. (2007): A parallel adaptive barotropic model of the atmosphere, J. Comp. Physics 223(2): 609-628, doi:10.1016/j.jcp.2006.09.029.
Laxon S., Peacock N. & Smith D. (2003): High interannual variability of sea ice thickness in the Arctic region.- Nature 425: 947-950.
Leck, C., Tjernström, M., Bigg, K., Matrai, P., & Swetlicki, E. (2004): Microbes, clouds and climate: can marine microorganisms influence the melting of the Arctic pack ice?.- Eos Trans. 85: 25-36.
Luo, L. et al. (2003): Effects of frozen soil on soil temperature, spring infiltration, and runoff: Results from the PILPS 2(d) experiment at Valdai, Russia.- J. Hydrometeorol. 4: 334-351.
Lynch, A.H., Chapman, W., Walsh, J.E., & Weller, G. (1995): Development of a regional climate model of the western Arctic.- J. Clim. 8: 1555-1570.
Maslanik J.A., Lynch, A.H., Serreze, M.C. & Wu, W. (2000): A case study of regional climate anomalies in the Arctic: Performance requirements for a coupled model.- J. Clim. 13: 383-401.
Maslanik, J., Drobot, S., Fowler, C., Emery, W. & Barry, R. (2007): On the Arctic climate paradox and the continuing role of atmospheric circulation in affecting sea ice conditions.- Geophys. Res. Lett. 34: L03711, doi:10.1029/2006GL028269.
Mahrt, L. (1998): Stratified atmospheric boundary layers and breakdown of models.- Theoret. Comput. Fluid Dynamics 11: 263-279.
Mikolajewicz, U., Sein, D.V., Jacob, D., Königk, T., Podzun, R. & Semmler, T. (2005): Simulating Arctic sea ice variability with a coupled regional atmosphere–ocean–sea ice model.- Meteorol. Z. 14: 793-800, doi:10.1127/0941-2948/2005/0083.
Monahan A.H., Fyfe, J.C. & Flato, G.M. (2000): Northern Hemisphere atmospheric variability and change under global warming.- Geophys. Res. Lett. 27: 1139-1142.
Palmer T.N. (1999): A nonlinear dynamical perspective on climate prediction.- J. Clim. 12: 575-591.
Perlwitz, J. & Harnik, N. (2003): Observational evidence of a stratospheric influence on the troposphere by planetary wave reflection.- J. Clim. 16: 3011-3026.
Perovich, D.K., Andreas, E.L., Curry, J.A., Eiken, H., Fairall, C.W., Grenfell, T.C., Guest, P.S., Intrieri, J., Kadko, D., Lindsay, R.W., McPhee, M.G., Morison, J., Moritz, R.E., Paulson, C.A., Pegau, W.S., Persson, P.O.G., Pinkel, R., Richter-Menge, J.A., Stanton, T., Stern, H., Sturm, M., Tucker III, W.B. & Uttal, T. (1999): Year on ice gives climate insights.- Eos Trans. 80: 483-486.
Perovich, D.K., Grenfell, T.C., Light, B., Richter-Menge, J.A., Sturm, M., Tucker III, W.B., Eicken, H., Maykut, G.A. & Elder, B. (1999): SHEBA: Snow and Ice Studies CD-ROM.- Cold Reg. Res. Eng. Lab., Hanover, N.H., Digital media.
Persson, P. Ola G., Fairall, C.W., Andreas, E.L., Guest, P.S. & Perovich, D.K. (2002): Measurements near the atmospheric surface flux group tower at SHEBA: near-surface conditions and surface energy budget.- J. Geophys. Res. 107: 8045, doi:10.1029/ 2000JC000705.
Proshutinsky, A., Dethloff, K., Doescher, R., Gascard, J.C. & Kauker, F. (2008): Toward reducing uncertainties in Arctic climate simulations.- Eos Trans. 89(16), doi:10.1029/2008EO160002.
Rinke, A., Gerdes, R., Dethloff, K., Kandlbinder, T., Karcher, M., Kauker, F., Frickenhaus, S., Köberle, C. & Hiller, W. (2003): A case study of the anomalous Arctic sea ice conditions during 1990: Insights from coupled and uncoupled regional climate model simulations.- J. Geophys. Res. 108(D9): 4275, doi:10.1029/2002JD003146.
Rinke, A., Dethloff, K. & Fortmann, M. (2004): Regional climate effects of Arctic Haze.- Geophys. Res. Lett. 31: L16202, doi:10.1029/2004GL020318.
Rinke, A., Dethloff, K., Cassano, J., Christensen, J.H., Curry, J.A., Haugen, J.E., Jacob, D., Jones, C., Køltzow, M., Lynch, A.H., Pfeifer, S., Serreze, M.C., Shaw, M.J., Tjernström, M., Wyser, K. & Zagar, M. (2006): Evaluation of an ensemble of Arctic regional climate models: Spatiotemporal fields during the SHEBA year, Clim. Dyn. 26: 459-472, doi:10.1007/s00382-005-0095-3.
Rinke, A., Kuhry, P. & Dethloff, K. (2008): Importance of a soil organic layer for Arctic climate-a sensitivity study with an Arctic RCM.- Geophys. Res. Lett. 35: L13709, doi:10.1029/2008GL034052.
Roeckner, E., Arpe, K., Bengtsson, L., Christoph, M., Claussen, M., Dümenil, L., Esch, M., Giorgetta, M., Schlese, and Schulzweida, U. (1996): The atmospheric general circulation model ECHAM-4: Model description and simulation of present-day climate.- MPI Rep. 218, Max Planck Inst. for Meteorol., Hamburg, 90 pp.
Saha, S.K., Rinke, A., Dethloff, K. & Kuhry, P. (2006): The influence of a complex land-surface scheme on Arctic climate simulations.- J. Geophys. Res. 111: D22104, doi:10.1029/2006JD007188.
Saha, S.K. Rinke, A. & Dethloff, K. (2006a): Future winter extreme temperature and precipitation events in the Arctic.- Geophys. Res. Lett. 33: L15818, doi:10.1029/2006GL026451.
Serreze M.C., Carse, F., Barry, R.G. & Rogers, J.C. (1997): Icelandic low cyclone activity: climatological features, linkages with the NAO, and relationships with recent changes in the northern hemisphere circulation.- J. Clim. 10: 453-464.
Serreze, M.C. & Francis, J.A. (2006): The Arctic amplification debate.- Clim. Change, doi:10.1007/s10584-005-9017-y.
Serreze, M.C., Holland, M.M. & Stroeve, J. (2007): Perspectives on the Arctic's shrinking sea-ice cover.- Science 315: 1533-1534.
Skeie, P. (2000): Meridional flow variability over the Nordic seas in the Arctic Oscillation framework.- Geophys. Res. Lett. 27: 2569-2572.
Sokolova, E. (2006): A study of large-scale atmospheric dynamics on the Basis of NCEP data and AOGCM simulations.- Diss. Thesis Univ. Potsdam, 128 pp.
Sokolova, E., Dethloff, K., Rinke, A. & Benkel, A. (2007): Planetary and synoptic scale adjustment of the Arctic atmosphere to sea-ice cover changes.- Geophys. Res. Lett. 34: L17816, doi:10.1029/2007GL030218.
Sorteberg, A. & Kvingedahl, B. (2006): Atmospheric forcing on the Barents Sea winter ice extent.- J. Clim. 19: 4772-4784.
Stenchikov, G., Hamilton, K., Stouffer, R.J., Robock, A., Ramaswamy, V., Santer, B. & Graf, G.-F. (2006): Arctic Oscillation response to volcanic eruptions in the IPCC AR4 climate models.- J. Geophys. Res. 111: D07107, doi:10.1029/2005JD006286.
Stendel, M., Christensen, J.H. & Mogensen, I. (2005): Influence of various forcings on global climate in historical times using a coupled atmosphere-ocean general circulation model.- Clim. Dyn. 25: 10.1007/s00382-005-0041-4.
Stenchikov, G., Robock, A., Ramaswamy, V., Schwarzkopf, M.D., Hamilton, K. & Ramachandran, S. (2002): Arctic Oscillation response to the 1991 Mount Pinatubo eruption: effects of volcanic aerosols and ozone depletion.- J. Geophys. Res. 107(D24), 4803, doi:10.1029/2002JD002090.
Stroeve J., Holland, M.M., Meier, W., Scambos, T. & Serreze, M. (2007): Arctic sea ice decline: faster than forecast.- Geophys. Res. Lett. 34: L09501, doi:10.1029/2007GL029703.
Thompson D.W.J., & Wallace, J.M. (1998): The Arctic Oscillation signature in the wintertime geopotential height and temperature fields.- Geophys Res. Lett. 25: 1297-1300.
Trenberth. K.E. & Hurrell, J.W. (1994): Decadal atmosphere–ocean variations in the Pacific.- Clim. Dyn. 9: 303-319.
Tjernström, M., Zagar M., Svensson G., Cassano J.J., Pfeifer S., Rinke A., Wyser K., Dethloff K., Jones C.G. & Semmler T. (2005): Modelling the Arctic boundary layer: an evaluation of six ARCMIP regional-scale models using data from the SHEBA project.- Boundary-layer Meteorol. 117: 337-381, doi:10.1007/s10546-004-7954-z.
van Lipzig, N.P.M., van Meijgaard, E. & Oerlemans, J. (2002): The spatial and temporal variability of the surface mass balance in Antarctica: results from a regional atmospheric climate model.- Int. J. Climatol. 22: 1197-1217.
Viterbo, P., Beljaars, A., Mahfouf, J.F. & Teixeira, J. (1999): The representation of soil moisture freezing and its impact on the stable boundary layer.- Q. J. Royal Meteorol. Soc. 125: 2401-2426.
Walsh, J.E., Lynch, A., Chapman, W. & Musgrave, D. 1993, A regional model for studies of atmosphere–ice–ocean interaction in the western Arctic.- Met. Atmos. Phys. 51: 179-194.
Walsh, J.E., & Timlin, M.S. (2003): Northern hemisphere sea-ice simulations by global climate models.- Polar Res. 22: 75-82.
Williamson, D.L., Drake, J.B., Hack, J.J., Jakob, R. & Swarztrauber, P.N. (1992): A standard test set for numerical approximations to the shallow water equations in spherical geometry.- J. Comp. Phys. 102: 211-224.
Wyser, K., Jones, C.G., Du, P., Girard, E., Willén, U., Cassano, J., Christensen, J.H., Curry, J.A., Dethloff, K., Haugen, J.-E., Jacob, D., Køltzow, M., Laprise, R., Lynch, A., Pfeifer, S., Rinke, A., Serreze, M., Shaw, M.J., Tjernström, M. & Zagar, M. (2007) An evaluation of Arctic cloud and radiation processes during the SHEBA year: simulation results from eight Arctic regional climate models.- Clim. Dyn. 15, doi:10.1007/S00382-007-0286-1.
Zhang, T., Heginbottom, J.A., Barry, R.E. & Brown, J. (2000): Further statistics on the distribution of permafrost and ground ice in the Northern Hemisphere.- J. Clim. 24: 126-131.
Zilitinkevich, S.S. (2002): Third-order transport due to internal waves and non-local turbulence in the stably stratified surface layer.- Q. J. Royal Meteorol. Soc. 128: 913-926.